JOURNAL OF MATERIALS SCIENCE 20 (1985) 1521–1555

Review
Ion sputtering and its biomedical applications. Theoretical concepts and practical consequences. Clinical implications and potential use

ZBIGNIEW W. KOWALSKI
Technical University of Wrocław, I-25, 50–370 Wrocław, Poland

It is the purpose of the paper to promote the ion beam sputtering technique and its biomedical applications among not only ion beam users but also other research workers, and especially, among biologists and medical doctors. The objectives of this article are threefold. Firstly, it supplies a conceptual background for discussing the main question of this work, i.e. biomedical applications of sputtering. Secondly, the title issue and some related problems, important in the biomedical use, are widely presented and discussed. Finally, clinical implication and potential applications are shown.

1. Introduction

The phenomenon, now called sputtering, was first observed in glass discharges by William R. Grove in 1852 and Faraday in 1854. It took about half a century until the physical process involved in sputtering was recognised and about 100 years until a quantitative description began to be developed. In recent years there has been a growing interest in the study of ion sputtering largely because of the practical applications of this process. Among them so-called "biomedical applications" are especially promising and useful. It appears that the technique in question can give two main biomedical applications:

(a) revealing of the subsurface features of biological derived materials resulting from ion sputter etching, and

(b) modification of the surface morphology of biocompatible materials induced by ion sputter texturing.

These unique capabilities of sputtering could potentially be used in cytological studies and in implantology. But this is the separate problem, which could be qualified as "clinical implication and potential applications of ion sputtering". It seems, that this difficult question should be studied first of all by medical specialists but, of course, with close co-operation with ion beam users.

The objectives of this paper are threefold. Firstly, it supplies a conceptual background for discussing the main problem of this work, i.e. biomedical applications of ion sputtering. This part of paper deals with theoretical concepts of sputtering, as well as experimental results and data. These problems are well known and exhaustively discussed in the suitable literature, and, therefore, only those are touched here, which are important and indispensable (from this article point of view). Secondly, the title issue, i.e. biomedical applications of ion sputtering and some related problems are widely presented and talked over. Finally, clinical implication and potential applications (as examples) are shown.

2. Sputtering by ion bombardment

Ion bombardment of solids causes a lot of events. One of them is ion sputtering. It is the purpose of this chapter to identify main events induced

0022–2461/85 $03.00 + .12

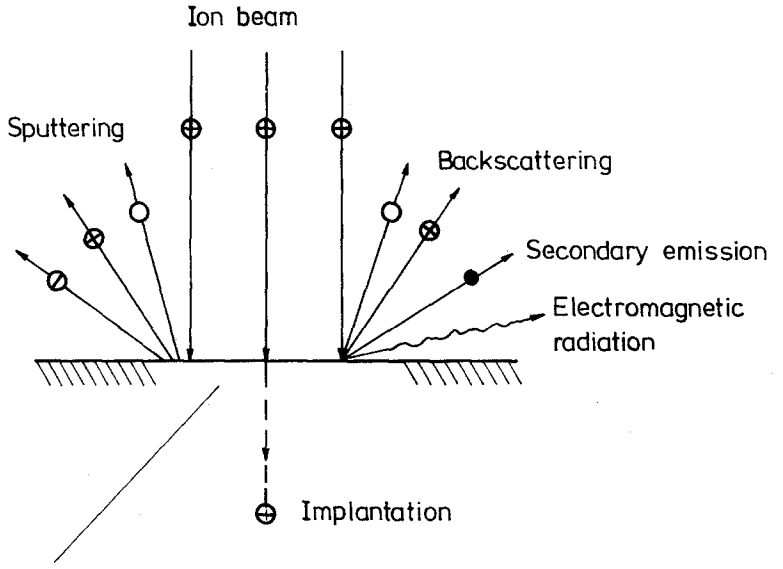

Figure 1 So-called target effects induced by ion bombardment of solids.

by ion irradiation and to present the most often measured sputtering parameter, i.e. the sputtering yield.

2.1. Identification of events

Bombardment of solids by energetic ions can result in several so-called target effects (see Fig. 1), i.e.:

1. Sputtering of energetic neutral target species with small amounts of secondary positive ions ($\sim 1\%$) and negative ions ($\sim 10^{-3}\%$) [1].
2. Backscattering of energetic ions and neutral atoms.
3. Emission of secondary electrons and electromagnetic radiation.
4. Ion implantation.

In addition to the effects mentioned above other processes (transport processes) may also be caused by ion irradiation. These are: (a) radiation damage, (b) diffusion, (c) cascade mixing and (d) segregation. Lastly, it is worth noting some derivative effects, such as: redeposition of sputtered material, changes of surface temperature, etc.

In this paper we will concentrate especially on the first effect, now called sputtering. This phenomenon is universal because all kinds of particles can erode all kinds of materials. Even light particles can give rise to considerable sputtering effects on certain types of target materials. Sigmund proposed a very useful definition of sputtering [2]. He believes that the four criteria are consistent with what is considered to belong to sputtering by most investigators:

1. Sputtering is a class of erosion phenomena observed on a material surface as a consequence of external or internal particle bombardment.
2. Sputtering is observable in the limit of small incident-particle current. It means that macroscopic heating and subsequent evaporation of a target by a high-intensity beam is not considered as a sputtering phenomenon.
3. Sputtering is observable in the limit of small incident-particle fluence. This criterion ensures that a single incident particle may indeed initiate a sputtering event. This separates blistering from sputtering phenomena.
4. Sputtering is observable on target materials of homogeneous composition. The criterion separates phenomena like collision-induced desorption from sputtering.

2.2. Sputtering yields

The most often measured parameter characterizing the sputtering process is the so-called sputtering yield. It is defined as the ratio of the average number of ejected to the number of incoming

particles. Sputtering may occur both from the bombarding side of the target (backsputtering) and from the side where the particle beam exists from the target (transmission sputtering). The corresponding yields are:

1. backsputtering yield, simply called the sputtering yield, and
2. transmission-sputtering yield.

It may be convenient at this point to note that the term "sputtering yield" is used in the literature to mean different things. Consequently, different types of sputtering yields have to be defined [3]:

1. The first, referring to pure and multicomponent materials, is the total sputtering yield Y, i.e. the number of sputtered atoms per incident particle. In the case of ions as incoming particles it is the number of sputtered atoms per ion.

2. The second coefficient is a partial sputtering yield Y_i of component i of a multiphase material. It can be defined as number of sputtered atoms of component i per incident particle (ion for example).

3. The next is a component sputtering yield Y_i^c, which is defined as the partial sputtering yield Y_i divided by the equilibrium surface concentration C_i^s of component i during sputtering. Both Y_i and Y_i^c are often denoted as the partial sputtering yield, but one has to clarify if either Y_i or Y_i^c is designated the partial sputtering yield.

The total, partial and component yields are related by:

$$Y = \Sigma_i Y_i \tag{1}$$

and

$$Y_i^c = Y_i / C_i^s \tag{2}$$

The sputtering yield depends on many factors [2], in particular on the type and state of the bombarded material [4–9] and the characteristics of the incident particle [10–25]. However, each factor does not influence the sputtering yield in the same way. For example, the effect of target temperature on the yield is, in general, small for temperatures not too close to the melting point. On the other hand, the surface topography may have a strong influence on the average sputtering yield.

Sputtering yield measurements have been performed for more than one hundred years, and a vast amount of data have been published [26, 27]. A necessary requirement for obtaining reproducible data is that the irradiation is performed in well-defined conditions with regard to the incoming beam, target material and vacuum (vacuum conditions may influence the target properties).

Among the variety of techniques of yield measurements one can distinguish four main methods, i.e.:

1. mass-change measurements,
2. thickness-change measurements,
3. microscopic measurements on the target, and
4. yield determination through analysis of surface composition.

Reliable experimental values of the sputtering yield lie in the region of 10^{-5} to 10^{3} atoms per incident particle [2].

2.3. Theoretical concepts of sputtering

2.3.1. Mechanisms of sputtering

Despite the universality of the ion sputtering phenomenon, a large variety of erosion mechanisms have been proposed during the past years. At the present time, we can say that no single erosion mechanism explains all experimental observations. Recently, Kelly [28] has classified six sputtering processes by considering the time scale, i.e. prompt and slow collisional processes, prompt and slow thermal processes, exfoliational sputtering, and finally, processes based on electronic transitions. From this point of view, when an incident particle hits the target surface at $t = 0$, prompt collisional processes involving direct or near direct particle–target interactions follow for $10^{-15} \leqslant t \leqslant 10^{-14}$ sec. One can recognize two groups of prompt collisional events characterized by uncorrelated collisons (i.e., rebound sputtering, recoil sputtering and reflection sputtering) and correlated collisions (bulk chains also known as focusons – typically 2 to 3 atoms in length). An ensemble of processes which are designated as slow collisional are caused by the cascade of moving target atoms and follow for $10^{-14} \leqslant t \leqslant 10^{-13}$ to 10^{-12} sec. Next, for 10^{-13} to $10^{-12} \leqslant t \leqslant 10^{-11}$ to 10^{-10} sec, occur prompt thermal processes, conventionally attributed to a thermal spike, and the recently recognized slow thermal processes, which occur for $t >> 10^{-11}$ to 10^{-10} sec (most notably the vaporization of alkali-metal atoms from the surfaces of alkali halides). Finally, for macroscopic times and at very high doses exfoliational sputtering, due to the rupture of gas filled cavities, sets in. Independently of this scheme one must also

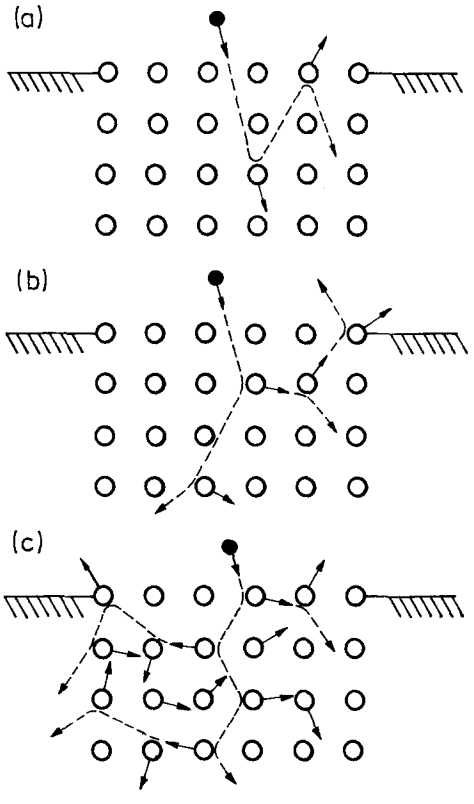

Figure 2 Three regimes of ion sputtering by elastic collisions [2]: (a) the single-knockon regime, (b) the linear cascade regime, (c) the spike regime. • Ion, ○ Target atom.

recognize the processes, which are fast ($t \leqslant 10^{-11}$ to 10^{-10} sec) or slow ($t \geqslant 10^{-11}$ to 10^{-10} sec) in nature, based on electronic transitions.

Slow collisional sputtering is often associated with the name of Sigmund [2, 12, 29–32] and is frequently the dominant mechanism with many, though not all, systems. According to his suggestions two main types of sputtering can be classified, i.e.:

1. sputtering by elastic collisions (knockon sputtering), and
2. sputtering by electronic excitation.

The elementary event of knockon sputtering is an atomic collision cascade, where the incident ion knocks target atoms off their equilibrium sites, thus causing these atoms to move and to undergo further collisions. Some of these atoms are ejected through the target surface (if energetic enough to overcome the binding forces). Knockon sputtering can be distinguished between three qualitatively different situations as shown in Fig. 2: (a) the single-knockon regime (lower and medium eV region; for very light ions – up into lower keV region), (b) the linear cascade regime (characteristic for keV and MeV ions, except for the heaviest ions which are stopped rapidly and tend to generate spikes), and (c) the spike regime.

In the single knockon regime, recoil atoms are energetic enough to get sputtered, but not energetic enough to generate secondary cascades. In the other two cases, they can generate secondary and even higher-generation cascades. The linear cascade differs from the spike regime in the spatial density of moving atoms, in spike regime this density is so high that the majority of atoms, within the so-called spike volume, are in motion.

The second type of sputtering is sputtering by electronic excitation. In insulators, excitation energy could be transferred to atomic motion because the lifetimes of the excited electronic states may be long enough to allow this. One may again consider three regimes, similar to those shown in Fig. 2 and presented above. For example, isolated in space ionizing or dissociating events may be generated by UV photons and low-energy electrons and/or ions. The linear ionization cascade and ionization spike regimes are pronounced in the cases of high-speed and heavy ions, respectively.

It is worth noting that within Sigmund's classification [2] chemical sputtering is a special case of sputtering by electronic processes. The traditional concepts of physical sputtering (i.e. ejection of target atoms through the surface resulting from kinetic energy transfer from the incident particles) and chemical sputtering (i.e. chemical reaction induced by the bombarding particles which produce unstable compounds at the target surface) might be abandoned for this reason. According to the Sigmund's theory the sputtering yield is proportional to the energy deposited at the solid surface, and is given by the formula:

$$Y(E) = 0.042 \frac{\alpha(M_2/M_1)}{U_s} S_n(E), \qquad (3)$$

where E is the incident projectile energy, U_s is the surface binding energy, usually taken to be equal to the sublimation energy, $S_n(E)$ is the nuclear stopping cross section, and $\alpha(M_2/M_1)$ is an energy-independent function of the mass ratio between the target mass M_2 and the ion mass M_1. Recently, however, definite systematic deviations from this formula have been pointed out for such cases as light-ion sputtering and low-energy

sputtering. Several attempts have been made to correct the above expression [2, 24, 25]. The angular dependence of the sputtering yield [12], especially in the case of light-ion sputtering and heavy-ion sputtering [25] has also been studied, and a simple empirical formula for preliminary description of this dependence has been proposed.

2.3.2. Some aspects of monocrystal sputtering

Comprehensive information about the ion sputtering of monocrystal targets relating to the theoretical aspects and experimental observations, measurements and data can be found in works of Robinson [33] and Roosendaal [27].

Experimental results have shown that the crystalline state of the target strongly influences the sputtering process of the material in question. "Monocrystalline effects" are revealed especially in: (a) sputtering yield measurements, and (b) the properties of the sputtered material, i.e. the angular distribution and energy spectra of sputtered particles. It has been stated that the sputtering yield for monocrystalline material is both a function of the ion incidence angle Θ as well as of the angle ψ with respect to the nearest low index direction. For the incidence of the ion beam along the low index crystallographic directions, the observed yield is generally lower than that for a polycrystalline target. As an explanation of the reduction in yield, the concept of channelling was introduced. It assumes the reduction of the collision probability for this part of particles which trajectories have a certain stability to remain near the centre of the channel (considered as the space formed by low index lattice rows). Strictly speaking, the idea of channelling assumes that channelled particles do not contribute to sputtering. Experimental observations have also shown that the angular distribution of particles sputtered from monocrystalline targets has distinct peaks for characteristic ejection directions. The energy distribution of the ejected particles are also significantly influenced by the crystalline structure of the sputtered target.

Several models of the ejection process from monocrystal surfaces have been developed throughout the years. It seems that neither of them can give more than a semiquantitative picture of the experimentally observed events. At present, no comprehensive theory exists. The main reason is probably the neglect of the full three-dimensional structure of the target crystals. Such a limitation can be overcome by computer simulation methods. But these methods are hampered by the lack of accurate models of surface crystal structure (i.e. for example the location of atoms, surface binding energy, etc.) and additionally are often very time-consuming and/or require large amounts of computer memory. Consequently, the largest and fastest computers must be used to produce statistically reliable quantitative results. In practice, more approximate and cheaper models are used and this is probably the main reason why the results are still far from being complete, and allow only a limited comparison with experimental data.

At the end of this section some words must be said about the importance of the surface preparation of the monocrystal targets [34]. When clean surfaces are used, the most dominant experimental parameters in studies of surface effects resulting from ion bombardment are the crystal lattice and orientation. In the case of poorly prepared surfaces, a lot of other effects, which completely obliterate the real physics of the sputtering process, must also be considered.

3. Material modification by ion sputtering

Ion sputtering of solid surfaces causes two major "material effects", i.e. (a) surface morphological changes, and (b) surface chemical alteration. They are discussed below. A short survey over theoretical models is also included because of its importance in understanding of the nature of morphological and compositional changes resulting from ion irradiation.

3.1. Surface morphological changes

The changes of surface morphology which occur as a consequence of ion sputtering have been studied for many years. The majority of the theoretical work has been concerned with random (amorphous) solids. In the subsequent discussion it may be convenient to distinguish between studies with:

1. random media where point and extended defects have little or no meaning, and the dominant effects will be a result of the macroscopic and microscopic variations of the sputtering yield as a function of the incidence angle and due to spatial variations of the energy deposition distribution near the point of ion impact, respectively, and
2. crystalline media where such effects may be

additional to that due to the microscopic scale variation in the sputtering yield as a result of defect production and interaction with the surface.

Each of the effects mentioned above may contribute in some way to the development of surface morphology, but other processes of atomic scale morphological change may also operate, especially processes such as: local sputtering yield variation [32], volume diffusion [35] and particle flux variation [36]. Several rather less important events must also be considered, i.e. the redeposition of sputtered material onto the closely adjacent planes, the ion reflection at grazing incidence, dechannelling at dislocation lines, modification of surface binding energy arising from variations in crystallographic orientation or elastic stress and sample temperature changes resulting from ion bombardment, etc. All these processes and/or events can result in significant deviations of the ion sputtered surface morphology from the theoretical predictions.

3.1.1. Survey over theoretical models

The first analysis of the surface topography modification induced by ion bombardment of the amorphous solids was made by Steward and Thompson [37] who investigated the motion of surface elements composed of intersecting semi-infinite planes. They, assuming that the dependence of the sputtering yield on the angle of ion incidence could possibly be responsible for the observed microscopic surface features, were the first to give the equation of motion of intersection of two planes during ion erosion. These results, applied to the step erosion, showed the dominant role played by the planes inclined at an angle Θ_m corresponding to the angle where the sputtering yield was a maximum (Θ is the angle between the beam incidence and surface normal). Erosion slowness theory confirmed [38] that, from an initially variously shaped surface the most probable and state orientations of the facets are normal and parallel to the ion beam direction. The model [35, 39–41], where the motion of individual points on a general two-dimensional surface was studied, has also shown that a steady state is reached when the surface topography consists of planes aligned either parallel or perpendicular to the direction of the ion beam and inclined at $\pm\Theta_m$. It should be noted, that similar results have been obtained in the model [42, 43] where a general surface contour was treated as an envelope of linear segments and where the time dependent behaviour of this envelope during erosion was investigated.

Experimental observations have shown, that during the ion bombardment of solid surfaces well-defined surface topographical features (undulations, waves) are developed. Several authors have tried to explain the formation of these features on crystalline surfaces suggesting [44, 45] that if a regular array of dislocations was formed by a defect agglomeration below the ion irradiated crystalline surface, then ion channelling would be interrrupted by these dislocations, the ion energy loss rate would increase locally near the surface, and a spatially periodic variation of sputtering yield would occur at the surface, giving rise to the regular features. Hermanne [45] has made a first attempt at defining the conditions for such dislocation growth and stability to occur. Another model [46] indicated that a regular dislocation array intersecting the surface or located beneath it may lead, in the first case, directly to a periodic variation of the surface binding energy or in the second case to a periodic variation of the surface stress, thus leading to periodic variation of the surface binding energy and thus of the sputtering yield and allowing surface undulations to form. It is worth noting that several attempts have also been made to develop computer models of surface topography evolution incorporating not only simple sputtering [47] but also ion reflection, redeposition, and surface diffusion [48].

Concluding this short survey we can say that:

1. An analytical approach, including computer simulation methods, to the development of surface morphology of random materials allows the prediction of trends in the surface development and prediction of the final steady-state contours. However, a complete analytical solution is generally unobtainable except for the simplest of contours. What the analytical approach does give, is a set of equations describing the instantaneous change of a surface contour over a short time interval.

2. There are several mechanisms by which regular structures can be initiated on solid surfaces (especially crystalline materials) during ion bombardment. However, whether any of these are themselves sufficient to account for the observed morphologies which develop after continued sputtering, is not clear.

TABLE I Topographical features most often observed at the bombarded surfaces of solids

Name of the feature	Kind of material sputtered	References
Cone	Metals, semiconductors, metal alloys, glass, resin	[32, 37, 39, 49–54]
Crater	Metals	[32, 44, 55]
Furrow or Groove	Metals	[32, 44, 56]
Hummock or Hillock	Glass, metals	[32, 39, 44, 52, 55]
Pit	Metals, semiconductors, glass	[39, 44, 49, 50, 54, 57]
Ridge	Metals	[32, 37, 53]
Step	Metals, semiconductors	[37, 39, 44]
Whisker	Semiconductors, resin	[49, 52]

3.1.2. Classification of morphological structures

Over the past years many topographical features have been observed at the ion bombarded surfaces but generally two types [45] or classes [49] of surface morphology or topography should be distinguished, according to their origin. One type consists of features of different aspects appearing on amorphous, polycrystalline and single-crystal surfaces, whose origin is related to impurities or irregularities present in or under the surface before the beginning of ion irradiation. Table I lists these features which are most often observed at the sputtered surfaces of solids.

The second type is more or less a regular pattern of arrays (e.g. parallel grooves, undulations) or any of the previous features appearing on the single-crystal surfaces or on the surface of only some grains of the polycrystalline samples. Their origin is related to radiation damage, i.e. the defects created and the impurities implanted during the bombardment. The regularity or randomness of this type of surface topography depends on the configuration of the extensive defects (formed by absorption of point defects), when the surface reaches their level.

The second class of surface topography can also be observed in the case of random solids but the mechanism of its formation is not clear. Table II presents, as an example, topographic features in question formed on the ion bombarded surfaces of glasses.

TABLE II Regular topographic features observed at the ion sputtered surfaces of glasses

Name of the feature	Kind of glass	References
Parallel grooves perpendicular to the beam	Natrium-calcium glass	[58]
Parallel grooves along the beam	Fused silica, Soda-glass	[52, 59]
Striated surface	Fused silica	[59]
Periodic strucutre	Glass	[46]
Waves	Corning 7059-glass	[60]

3.2. Surface chemical modification

In addition to surface morphology changes the ion bombardment can also modify the surface and/or subsurface chemical composition of the solids (properly multicomponent materials, i.e. materials consisting of more than one element). This is indicated in the work of several investigators [3, 61–75]. In the subsequent discussion it may be convenient to classify the multicomponent materials according to their structure (Fig. 3). They can be distinguished as:

1. single-phase materials which are characterized by having the same composition of elements uniformly distributed, and
2. multiphase materials, i.e. heterogeneous systems consisting of different crystallites which represent different phases, compositions and sometimes crystal structure (e.g. the majority of alloys, mixtures of different materials).

According to the specific responses to ion bombardment single-phase materials can be divided into the following three sections:

1. single-phase alloys,
2. single-phase compounds with no high vapour pressure components (e.g. silicides, carbides, semiconductors, intermetallic compounds) and
3. single-phase compounds having high vapour pressure components (e.g. oxides, nitrides, halides).

In spite of the large amount of experiments performed up to the present, the sputtering process for multiphase materials is not fully understood and a large amount of data, mainly for higher ion fluences, are difficult to understand [3]. In the present state of knowledge it is rather impossible

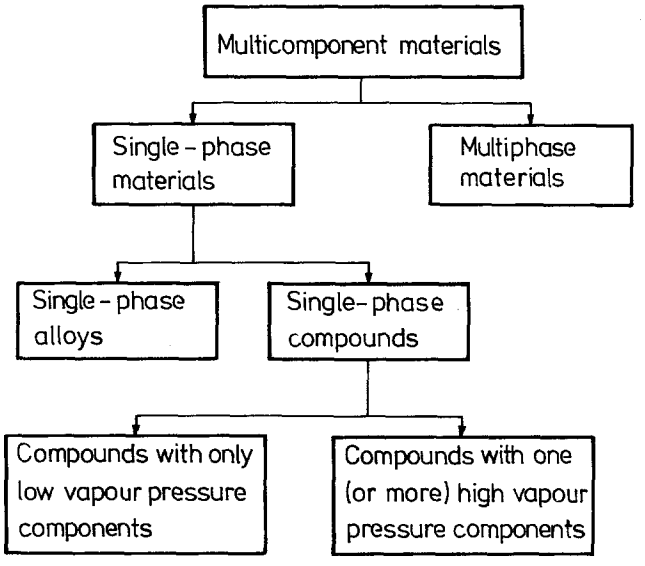

Figure 3 Classification of the multicomponent materials considered and practically used as ion bombarded targets.

to draw any general conclusions. It seems that further experiments under well-defined conditions are needed. While for the systems in question the theoretical conceptions are "premature", this is not the case for single-phase materials. Theoretical concepts and experimental results concerning the ion bombardment of single-phase systems are presented in the next two sections.

3.2.1. Processes and models

The large number of experimental results obtained from ion bombardment of single-phase materials enables the processes which contribute to the observed composition changes to be distinguished. It has been stated that various components are generally not sputtered proportional to their surface concentration. This phenomenon is now called preferential sputtering and means the different ejection probabilities of the different target components.

Ion bombardment leads generally to surface enrichment of the component having a lower sputtering yield. Conceptually, if one of the components has a significantly different sputtering yield than the other, the element with the higher yield will be preferentially depleted from the target surface leaving the other elements enriched. It is worth noting that the term "sputtering yield" is used in the literature to mean separate things. Three major definitions have been presented in section 2.2.

One important question in sputtering studies is the correlation of the sputtering yield in multicomponent materials with those of the pure elements. Generally, the preferential sputtering behaviour of these materials cannot be predicted according to the sputtering yields of individual elements. Also total sputtering yields of multicomponent systems have been found to be quite different from a superposition of the yields of the components. On the other hand, the experimental results show for some multicomponent materials, especially for single-phase metal alloys, that observed surface enrichment is in agreement with sputtering yields of the pure elements, i.e. that the component with the lower elemental yield becomes enriched under ion irradiation [3]. Although the sputtering yield studies are very useful and necessary they do not directly contribute to understanding the mechanism of the preferential sputtering of multicomponent systems. The main reason is that the sputtering yield is the phenomenological coefficient [76] and it depends on many factors. It is very important that to well-known sputtering parameters (such as: mass and kind of ions, their energy and incidence angle, the mass and kind of target atoms, crystal structure and orientation in the target material, and the binding energy of atoms to the surface) some new factors must be added, when multicomponent materials are considered [74], i.e. ion dose, target temperature, a binding energy which becomes dependent on concentration of the components, the evolving surface topography and the properties as derived from the phase diagram of the material.

For multicomponent systems, the effects of component mass difference and binding energy

seem to be of fundamental importance for understanding the nature of the preferential sputtering mechanism. Over the whole period lively controversies have been going on between the supporters of these two factors. At the present time, the general consensus is that both, differences in the mass and in the surface binding energy of the constituents, are very important but the binding energy seems to play the dominant important role. This clearly results from the tables of experimental data compiled from about 250 references by Betz [3]. Only in the single knockon regime and for systems with quite different masses for the constituents, mass effects clearly dominate, i.e. the lighter species are preferentially sputtered.

The thickness of the surface layer modified by ion bombardment, the so-called "altered layer", is mostly comparable to the range of the incident ions (depth of ion penetration). This is much greater than the thickness of the layer from which the atoms are sputtered, i.e. than could be expected from preferential sputtering itself. Therefore some other processes (called bulk, transport or secondary processes) must be considered in addition to the preferential sputtering such as:

1. thermal diffusion,
2. radiation enhanced diffusion,
3. recoil implantation,
4. cascade mixing,
5. thermal surface segregation, and
6. radiation enhanced segregation.

Thermal diffusion can give compositional changes over a depth much greater than the range of the primary particles. On the other hand, it seems that the diffusion enhancement is rather small in the ion bombardment induced compositional changes at room temperatures [62]. Ion irradiation can also modify the second diffusion process, i.e. radiation enhanced diffusion. Under this irradiation many lattice atoms are displaced, creating point and larger defects, which all increase diffusion. Diffusion processes can only counteract compositional changes resulting from preferential sputtering. They simply randomize the target material.

Collisional processes such as recoil implantation and cascade mixing can give changes of chemical composition over the depth of the collision cascade. Recoil implantation causes enrichment of the heavy species near the surface, while the lighter species tends to transport deeper into the target. The basic phenomenon of cascade mixing is not yet well understood but several models have been developed [77, 78]. The process in question, just as with diffusion, tends to smear the concentration gradients generated by preferential sputtering and recoil implantation.

The last group of secondary processes are segregation processes, which may produce different phases both, at the target surface and in the deeper layers, preventing a stationary state to develop.

It must be said at this point that the relative significance of the bulk processes for observed compositional changes in various multicomponent materials has not yet been clarified.

The ion bombardment of single-phase

TABLE III Principal characteristic of the instruments for the analysis of surfaces*

Analysis technique		Method of excitation	Analysed particles	Analysed value	Obtained information
Full name	Abbreviation				
Auger electron spectroscopy	AES	Electrons	Auger electrons	Energy	Composition of the altered layer as a function of depth
Electron spectroscopy for chemical analysis or X-ray photoelectron spectroscopy	ESCA or XPS	X-rays	Electrons	Energy	As above
Ion scattering spectroscopy	ISS	Ions	Backscattered ions	Energy	Composition of very outermost surface layer
Rutherford backscattering spectrometry	RBS	MeV ions	As above	Energy	Altered layer studies, information about its depth

*For further information, see Holland *et al.* [1], pp. 349–368.

TABLE IV Survey over ion sputtered single-phase systems analysed with AES, ESCA, ISS and RBS

Analysis method	Ion energy, energy range* (keV)	Kind of bombarding ions	System analysed and references		
			Single-phase alloys	Compounds with only low vapour pressure components	Compounds with only one high vapour pressure component
AES	0.3–5	Ar	Ag–Au [64, 66, 72, 79, 80], Ag–Cu [72], Ag–Pd [12, 64, 66, 81, 82], Al–Cu [83], Au–Pd [12, 64, 66, 84] Cu–Au [64, 72, 79], Cu–Ni [85–87] Cu–Pd [12, 64], Cu–Pt [64], Fe–Cr [88, 89], Ni–Cr [88], Ni–Fe [88–89], Ni–Pt [64], Pb–In [90], Pd–Ni [81], Pd–Pt [91], Ag–Au–Cu [72], Ag–Au–Pd [66], Fe–Cr–Ni [88]	AlAu, $AlAu_2$, $AlCr_2$, AlFe and $AlNi_3$ [89, 97], AuSn [98], Cu_3Sn and Cu_6Sn_5 [99], GaAs (1 0 0)–[100], GaAs [101], InSb(1 0 0)–[102], PtSn and Pt_3Sn [103], SiC [104] TiC [105]	Al_2O_3 and BeO [106], Ga_2O_3 [107], MgO [105, 108], MoS_2 [109], Si_3N_4 [110], SiO_2 [102], Ta_2O_5 [112], TiO_2 [112, 113]
		H		SiC [104]	
		He			Al_2O_3 and BeO [106], Ta_2O_5 [111]
		Xe	Cu–Pt [64], Ni–Pt [64], Al–Cu [83]		
		Ne, Xe		AlAu, $AlAu_2$, $AlCr_2$, AlFe and $AlNi_3$ [89, 97]	
		Ne, Kr, Xe		InSb (1 0 0)–[102]	
ESCA	0.2–1	Ar		GaAs (1 1 1)–[114]	PdO [115]
	0.4–5		Ni–Fe [95], Fe–Cr–Ni (304SS) [95]		Ag_2O, Ag_2O_2, Al_2O_3 and Au_2O_3 [115], Bi_2O_3 [116], CdO [115], $Co(CN)_2$ and CoF_2 [117], $CoFe_2O_4$ [118, 119], CoO [118, 120], Co_2O_3 [121], Co_3O_4 [118, 120], $Co(OH)_2$ [118], CoS [122], Cr_2O_3 [115, 123], CuCN [117], CuCl and $CuCl_2$ [117, 124], CuF_2 [117, 124, 125], CuO [115, 125], Cu_2O [115], CuS [122], FeF_2 [117, 125], FeO [115, 118, 119, 126], FeOOH [118, 126], Fe_2O_3 [115, 118, 119, 125, 126], Fe_3O_4 [118, 119, 123, 126], $FeSO_4$, FeS and FeS_2 [124], IrO_2 [115], $KMnO_4$, $LaCoO_3$, $LaSr(CoO_3)_2$ and MnO_2 [121], MoO_3 [115, 116], $Ni(CN)_2$ and NiF_2 [117], NiO [115, 123, 127], Ni_2O_3 [115, 127], Ni(OH) [115,

					118, 123], NiS [122], PbO [115, 128], PbO_2 and RuO_2 [115], SiO_2 [115, 116, 129], SnO_2 [115], $SrMnO_3$ [121], Ta_2O_5 [70, 115, 116], TiO_2 [116], Ti_2O_3 and WO_2 [115], WO_3 [115, 116], ZnF_2 [117], ZnO [115], ZnS [122], ZrO_2 [116]
		Ar, N_2	Ag–Pd [96]		
		O_2			Au_2O_3 [115], NiO [127], RuO_2 [115]
		He			PbO [128], Ta_2O_5 [130]
	10	Ar			K_2PtCl_4 and K_2PtCl_6 [131]
ISS	0.3–5	He, Ar			Al_2O_3 and BeO [106], Ta_2O_5 [111, 130]
and/or		Ne	Ag–Au [96]		
AES	0.2–8	H, D, He, Ne, Ar		TaC [106, 132, 133], WC [106, 132–135]	
RBS	1–2	Ar, Xe	Al–Cu [83]		SiO_2 [136]
	10–40				LiF [137]
	50	Ne			$PdCl_2$ [138]
	20–85	Ne, Ar, Kr, Xe	Cu_3Au [93, 94]	Al_2Au, $AlAu_2$ and GeSi [94], GaP [94, 139], InP, NiSi and Pt_2Si [94], PtSi [94, 140, 141]	Ta_2O_5 [94, 142]
	15–200	Ar	Ag–Au [93]		

*This is the maximum energy range which contains individual ion energies used by the referred authors.

compounds having high vapour pressure components may result in several "new" events, causing other mechanisms to be considered in addition to those mentioned above (i.e. for single-phase alloys and compounds with no high vapour pressure components). Four of those events seem to be of great importance, i.e.:

1. breaking or forming of new chemical bonds,
2. modification of the crystalline structure,
3. amorphization and/or crystallization of a near surface layer, for oxides and other nonmetalic compounds, and
4. reduction of the oxide to the more metallic state (it was found for multitude of oxides [3], that oxygen is lost preferentially).

About 150 examples of single-phase materials which were ion sputtered and analysed by surface analysis techniques, all with suitable references, are presented in the next section.

3.2.2. Experimental techniques and results

To investigate new important events induced by ion bombardment of multicomponent systems, to understand the mechanisms of surface composition changes, and finally, to develop adequate model of sputtering of the materials in question, it is necessary to obtain a lot of independent experimental results. Access to reliable suitable data only became possible with the development of surface analysis techniques, such as Auger electron spectroscopy (AES), electron spectroscopy for chemical analysis (ESCA) also known as X-ray photoelectron spectroscopy (XPS), ion scattering spectroscopy (ISS) or Rutherford backscattering spectrometry (RBS). These four methods have been widely used in the study of the altered layer at the surface of various multicomponent materials. Sometimes, in addition to those other techniques, such as low (LEED) and high (HEED) energy electron diffraction as well as energy distribution measurements (EDM) were also utilized, especially for compounds with one high vapour pressure component. Principal characteristics of AES, ESCA, ISS and RBS, i.e. the techniques usually used for surface analysis of ion treated single-phase materials, are presented in Table III. Table IV gives a survey over the ion sputtered systems studied in recent years with the techniques mentioned above. In addition, suitable information about the kind and the energy of the bombarding ions used for sputtering of each system, as well as numerous references (which may give more exact data) are also given. This compilation of data and references has been greatly facilitated by the existence of the tables on surface composition changes by Betz in the preliminary version of reference [3]. The present survey shows that the most commonly utilized techniques are Auger electron spectroscopy and electron spectroscopy for chemical analysis. The latter method was applied especially to compounds with only one high vapour pressure component, i.e. to oxides, nitrides, halides. Precise data about the modification of surface composition resulting from ion bombardment of single-phase systems can be found in reference [3].

4. Biomedical application of sputtering

Unique capabilities of ion sputtering enable this process to be applied in the field of biomedicine [143–154]. It seems that two main biomedical applications could be distinguished according to the sputtering processes used in the experiment (Fig. 4). The first process is sputter etching, i.e. the removal of material atoms from the surface by energetic ions and/or neutral particles which bombard the target. The second is sputter texturing which means microroughening of the irradiated surface due to spatial variations in sputtering yield of the target surface. It must be stated that sputter etching is the situation where texturing is undesirable but, unfortunately, it usually exists. It is important, in this case, to understand the nature of surface texturing to be able to suppress the development of the texture. Using ion sputter etching, it is possible to reveal the internal structure of biologically derived materials, such as for example; cells and soft or hard tissues. Sputter texturing is the process which can modify the surface texture of various biomaterials (biocompatible materials), such as for instance: biological implants, prostheses, artificial organs, assist devices, cell attachment testers, etc.

The third sputtering process, i.e. sputter deposition is beyond the scope of this article and, therefore, it is not discussed here.

4.1. Revealing the internal structure of biologically derived materials

Ion sputter etching in combination with scanning electron microscopy gives rise to the very interesting possibility of structural studies of various materials.

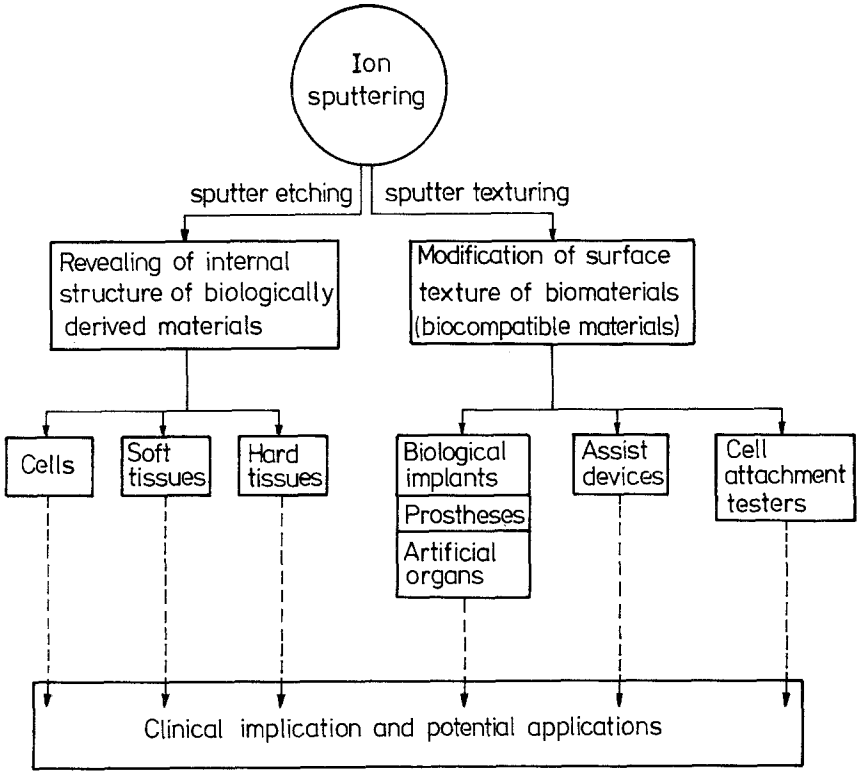

Figure 4 Biomedical application of ion sputtering.

It is well known that the crystalline state of the target strongly influences the sputtering process, especially the sputtering yield. It means that the grains with different crystal orientation are etched with different sputtering rates and, consequently, that they can be revealed during ion irradiation. Fig. 5 shows, as an example, the sputtered surface of an Fe–Mo alloy with distinctly visible grains [155], which were disclosed from an initially smooth surface during ion bombardment from a duoplasmatron source.

In the last two decades several attempts have been made to reveal the internal structure of biologically derived materials. Experimental studies have been concentrated on three major kinds of these materials:

1. biological cells (human [143–145] and avian [146] red blood cells, mammalian cells [146], viruses and bacteriophages [147]),
2. soft tissues (e.g. rat duodenum [52]), and
3. hard tissues (human teeth [52, 148]).

Preliminary findings have demonstrated the potential value of ion etching in studying the structure of normal and pathological red blood cells and other soft tissues [52, 144]. However, contrary to these optimistic opinions, there have been some difficulties in distinguishing intercellular structures from artefacts produced by the ion processing. It has been shown that ion sputtering (etching) may create a lot of topographical features on the ion irradiated surfaces; examples are presented in Tables I and II. This is a result of very complicated phenomena (described in previous sections) involved in this process.

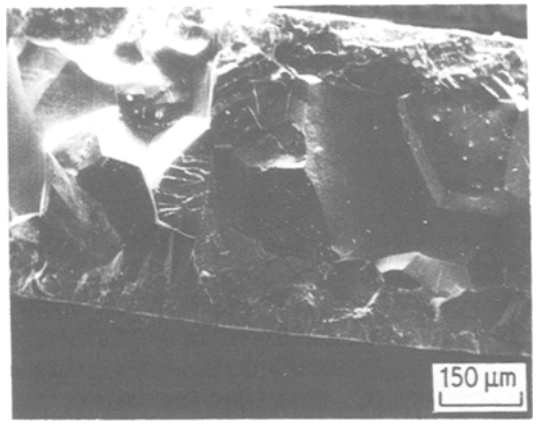

Figure 5 Grains revealed by ion sputter etching of Fe–Mo alloy.

The situation is more difficult in the case of biologically derived materials, especially soft tissues and cells, where the mechanism of creation of the artefacts in question is almost unknown. In spite of these pessimistic results, ion etching seems to be a good tool in revealing these organelles in the cytoplasm or these parts of the tissue which are characterized by low sputtering yields (which are etch-resistant). For example, this technique has allowed some insight to be gained into the orientation of the nucleic acid within a virus [147] or into the pulp of the tooth [52]. It is also a very good method for the study of dental materials, and especially the enamel/restoration interface. The problem of microleakage around dental restorations is of great importance. It appears that although good adaptation between restorative material and enamel is indicated on the surface, this is in fact not the case down the whole depth of the cavity wall [148]. This very short survey of the experiments indicates that sputter-etching can successfully be applied to some but not all, biologically derived materials. On the other hand, the inability to distinguish cellular structures from features produced by the ion etching suggests that a better understanding of the ion sputtering of the organic materials is required. This means that further investigation should be expected.

4.2. Modification of surface morphology of biomaterials (biocompatible materials)

Sputter etching used to reveal the internal structure of biologically derived materials preferentially etches them in ways similar to chemical etching. However, under a variety of conditions ion sputtering can produce a textured surface consisting of several kinds of features including cones, hillocks, hummocks, pits and other structures presented in Tables I and II. This process is usually referred to as sputter texturing or simply, texturing.

Ion beam texturing has been tested with different material combinations and has several potential applications. Among them biomedical use is probably one of the most promising. Three major sputter texturing techniques usually applied to modification of surface morphology of various biomaterials (biocompatible materials) could be distinguished, i.e. natural texturing (NTex), seed texturing (STex) and pattern texturing (PTex). The microscopically rough surface texture produced by these techniques may result in improvements in biological response and/or performance of implanted devices. In addition to morphology changes, which are predominant, ion bombardment modifies the chemical composition of sputtered biomaterials (biocompatible materials) and therefore it is not easy to attribute alterations in the mechanical properties of these materials and/or in the tissue response data to one or other cause. It seems that additional studies are necessary to answer these difficult questions. For example, the use of transfer cast biopolymers peeled from ion beam textured (pattern textured) surfaces may allow morphological changes to be fabricated with minimal or no surface chemical alteration [150]. Ion beam texturing techniques usually applied to biomaterials, as well as problems of ion bombardment induced compositional and mechanical changes are presented and discussed in the next two sections.

4.2.1. Surface texturing techniques

4.2.1.1. Natural texturing. Natural texturing (NTex) is the microroughening of the ion bombarded surface of the sample that occurs if there are spatial variations in the sputtering yield of the target surface (Fig. 6). The above definition is very simple and convenient because it clearly shows the major properties of the NTex technique which distinguish natural texturing from other possible techniques. Unfortunately, the definition cannot give "the full picture" of the creation of the surface texture, for this is a very complicated phenomenon and many events may contribute in some way to this texture development. Different types of materials can develop natural texture as a consequence of ion bombardment. In the last years various biomaterials and

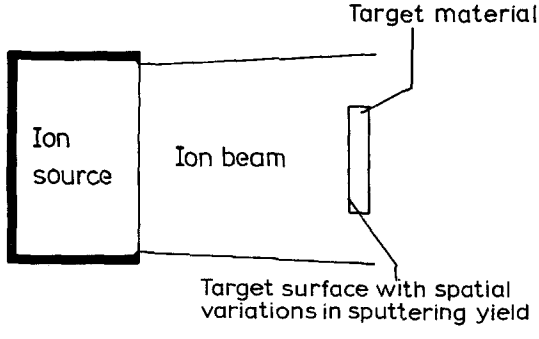

Figure 6 Schematic representation of natural texturing of the solid surface.

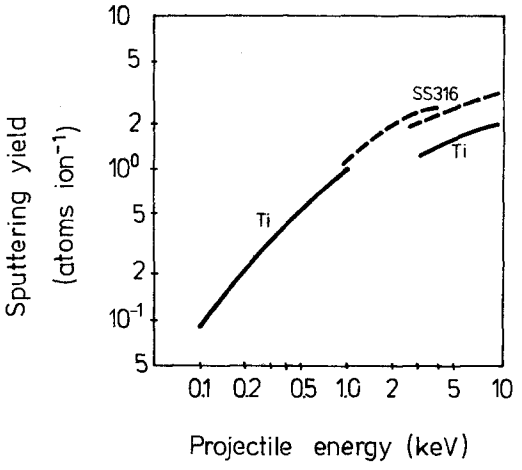

Figure 7 Experimental sputtering yields for titanium and SS 316 stainless steel targets (data from Andersen and Bay [26]).

biocompatible materials, such as, metals, alloys, polymers and ceramics, have been ion sputtered with various types of ion sources and then examined by scanning electron microscopy [149, 150, 156–160]. Experimental results have shown that ion sputtering can texture surfaces of the materials in question in a different manner according to the particular properties of the materials, as well as the sputtering conditions, e.g. ion energy, its angle of incidence, time of ion bombardment, used in the experiment. SEM images showing the ion sputter induced surface texture of four selected biomaterials and biocompatible materials (each from the other group of materials, i.e. from metals, alloys, polymers and ceramics) are presented and discussed below. The selected materials are: titanium, chrome–nickel stainless steel, polyester and alumina ceramic. Titanium has been chosen because, among other things, it is good material for dental implants. It was tested as an endosteal blade vent implant [149, 150]. The next two biomaterials, i.e. chrome–nickel stainless steel and polyester were utilized for orthopaedic (see for example Catalogue of OSTEO AG, Selzach products, 1976) and vascular [158] implants, respectively. Alumina, chosen as a representative of ceramics, is a very interesting material because it is used both, as substrate for thick film circuits and recently as artificial bone [161, 162]. Suitable data relating to the etch rates and sputtering yields of the selected materials are presented in Table V and Fig. 7, respectively. The influence of texturing on their surface morphology is shown in the following photomicrographs. Fig. 8 shows the surface of polycrystalline 99.9% titanium before (Fig. 8a) and

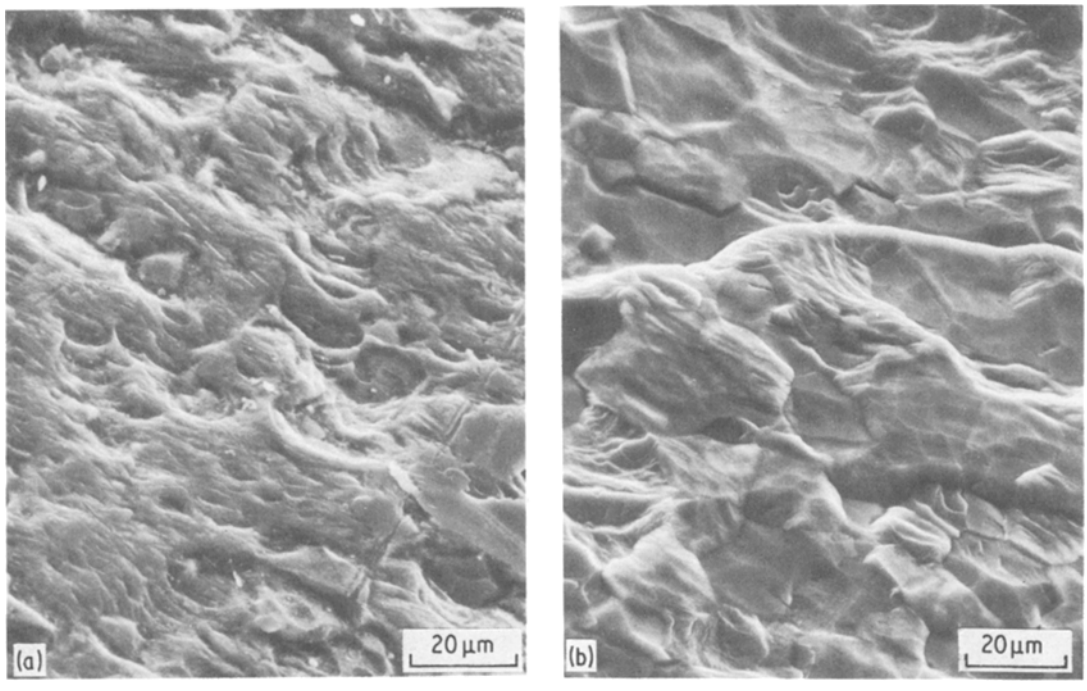

Figure 8 Titanium surface topography [159, 160], (a) before, and (b) after 210 min of natural texturing at an accelerating voltage of 1000 eV and beam current density of 2 mA cm^{-2}.

TABLE V Etch rates of alumina, stainless steel and titanium for normal argon ion beam incidence

Material	Etch rate (nm min^{-1})	
	1 mA cm^{-2}	2 mA cm^{-2}
	500 eV	1000 eV
Alumina	8–12	50–70
Stainless steel 304 or 316	25	140 max
Titanium	13–35	95 max

For further information see Kowalski and Rangelow [159]

after natural texturing (Fig. 8b) for 210 min with the aid of Kaufman type source. The initial, unsputtered, surface was altered during ion bombardment with an inclination to creating larger topographical features and to obliterating various pits, holes or craters. In isolated areas of the textured surface individual grains were revealed and also waves could be observed. The influence of NTex on morphology changes is more distinctly visible in Fig. 9, where SEM images of untreated (Fig. 9a) and ion sputtered (Figs. 9b to d) surfaces of chrome–nickel stainless steel are presented. This steel (17.5% chromium, 12.5% nickel, 3% molybdenum, and 0.03% max carbon) corresponds to the American standard AISI 316 LC or the German material number 4435. The unsputtered surface was almost smooth. Only a few pits with inclusions of grinding compound and some flaws, after polishing, could be seen. After ion bombardment from a Kaufman type source the initial smooth surface changed with a tendency to roughening (Fig. 9b). Flat planes with single pits and areas with periodic structure, parallel grooves, were dominant topographical features. Sporadically isolated pits with inclusions could also be observed. The ion sputtered surface became more textured, the surface roughness increased, and the topography was distinctly visible as the sputtering duration increased (see Figs. 9b and c). In spite of self-evident differences in surface morphology, both surfaces in question have a very similar character, or nature. It is impossible to say this about the third surface of chrome–nickel stainless steel which was ion irradiated from a glow discharge ion gun with a hollow anode (Fig. 9d). The surface texture has a different character and looks like desert sand or quicksand with shallow pits, isolated holes, steps and terraces. Other texturing effects (e.g. shadowing) and topographical features result from natural texturing of polymers. Fig. 10 shows a SEM image of polyester Symbol 10 (made in Poland) after argon ion beam bombardment [158]. Polyester is an elastic polymer used for vascular implants; they are made of knitted polyester material consisting of COOR groups, where C is carbon, O is oxygen, and R is the organic radical. The bombardment region of the polymer sample had a matt black appearance to the eye, probably due to an increase of carbon on the sputtered surface. It is clearly seen from the picture that during ion irradiation some synthetic fibres (threads) were partially shadowed by others. As a result of shadowing, parts of the fibres were not sputtered and remained smooth and "thick" (untreated threads had greater diameters than ion textured threads). The effect of ion bombardment on the polyester surface texture is presented in Fig. 11. The unsputtered surface (Fig. 11a) was found to be almost completely smooth. After ion irradiation a dense mass of whiskers, very irregular in shape, could be observed on the surface of the fibres (Fig. 11b). It is difficult to say anything definite to explain the mechanism of sputter texturing of polyester material. Only, several possible mechanisms could be considered:

1. ion sputtering of COOR molecules,
2. ion sputtering of polyester material, with different sputtering ratios for C, O and R, and
3. ion sputtering of polyester material and/or chemical decomposition of the material.

The observed surface texture (Fig. 11b) is probably due to the differences between the sputtering yields of carbon, which has an extremely low sputtering yield, and the rest of the chemical elements, of the polymer.

The next group of non-conductive materials which were successfully textured are ceramics and among them alumina ceramic [157–159, 163–165]. Fig. 12 represents the surface of 96% alumina before (Fig. 12a) and after (Fig. 12b) natural texturing with the aid of a hollow anode gun. As opposed to the polyester material, the untreated surface of alumina was not smooth – differently shaped and oriented grains were visible. These grains were not seen after irradiation. The initial topography changed with a tendency to smoothing but simultaneously microroughening occurred due to preferential sputtering of the

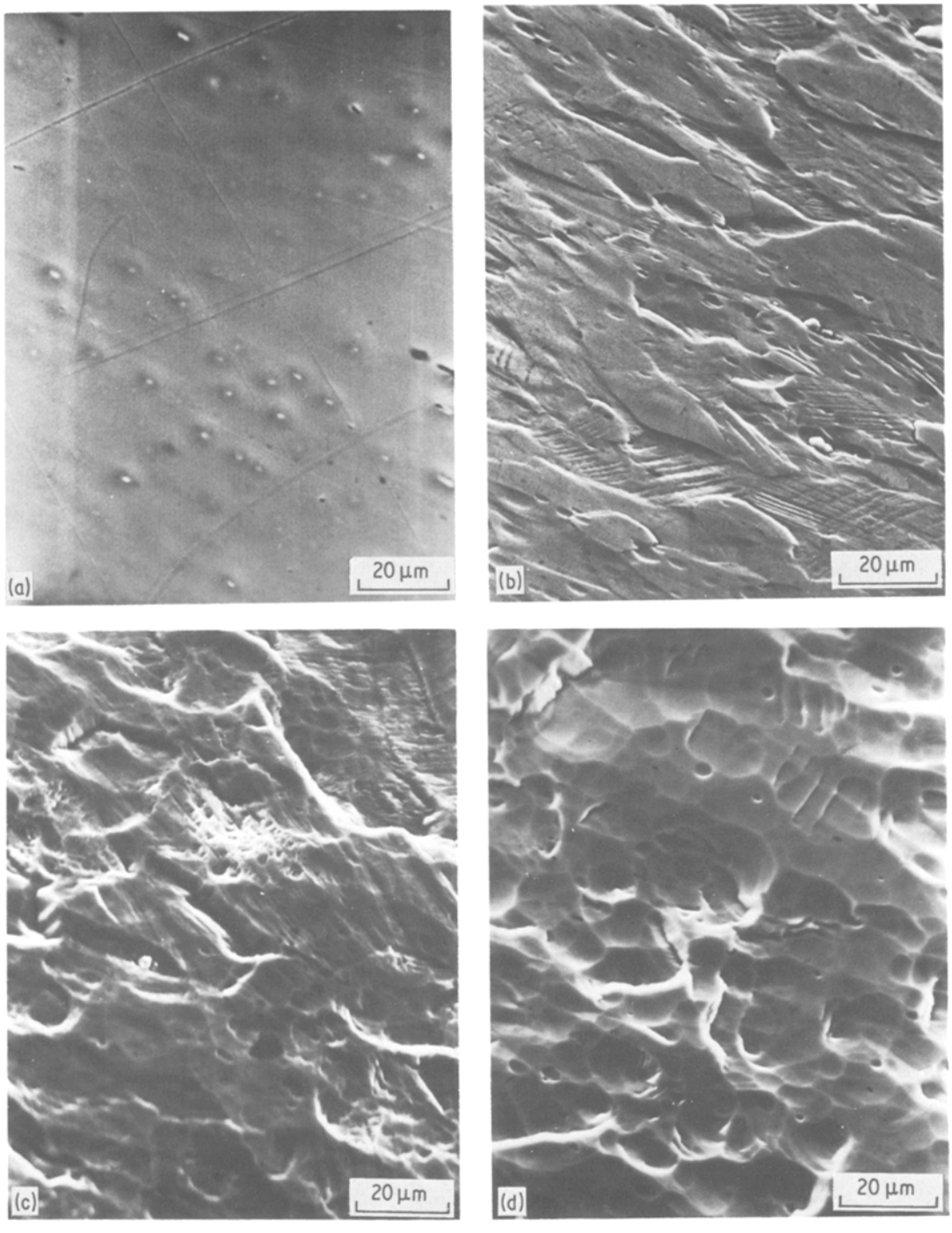

Figure 9 Scanning electron photomicrographs of chrome–nickel stainless steel [158, 159], (a) before ion irradiation, (b) after natural texturing for 50 min at an accelerating voltage of 1000 eV and beam current density of about 1 mA cm^{-2}, (c) after NTex for 600 min at the same voltage and similar beam current density, and (d) after 200 min of texturing at an accelerating voltage of 7 kV and total beam current of about 70 μA.

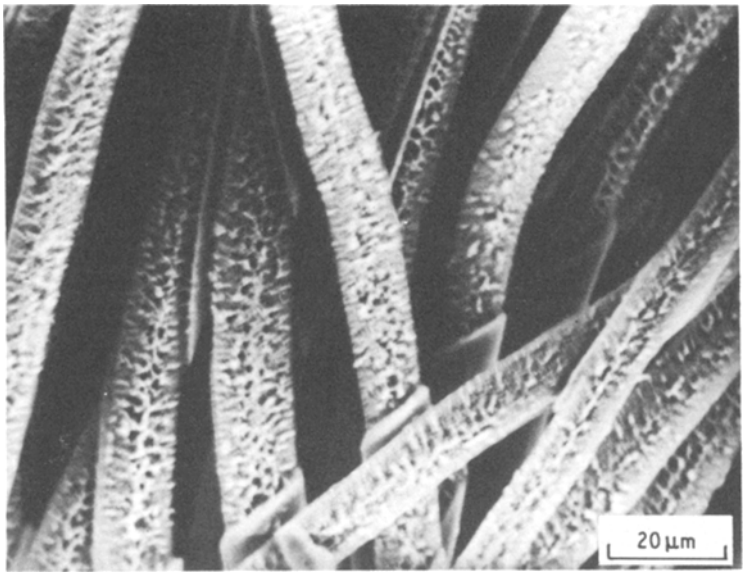

Figure 10 SEM image of polyester material after 90 min of natural texturing [158] at an accelerating voltage of 7 kV (the hollow anode ion gun was used as an ion beam source).

pore walls and a large angular dependence of the sputtering yield. Both these processes determined the final state of the surface roughness and topography. The sputtering process could be considered as the erosion of the ion impact amorphized homogeneous and isotropic material containing pores and inclusions [166]. This can be observed in Fig. 12b, where the natural textured surface of alumina shows a great number of flat shaped cavities; sputtering revealed deep pores and single inclusions, but without any signs of grains and grain boundaries. Ion bombardment can modify the alumina surface morphology very quickly. To prove this, to compare the irradiated surface topography with that of the initial surface or, eventually, to measure the removal material thickness, the sample can be partially screened with a mask during ion irradiation. The border between the textured and untreated surface obtained after bombardment of alumina sample partially screened with molybdenum foil is shown in Fig. 13. As can be seen, the surface morphology has been modified even if the ion dose was relatively small and the thickness of material layer removed by sputtering was too small to be measured. Grains considered as "semicircular profiled" surface elements (upper part of the image) were changed into "triangular shaped" features, which is consistent with results obtained by computer simulation of the line edge profiles undergoing ion bombardment [47, 48].

All the surface textures presented and discussed up to here were developed on different biomaterials under perpendicular ion beam bombardment.

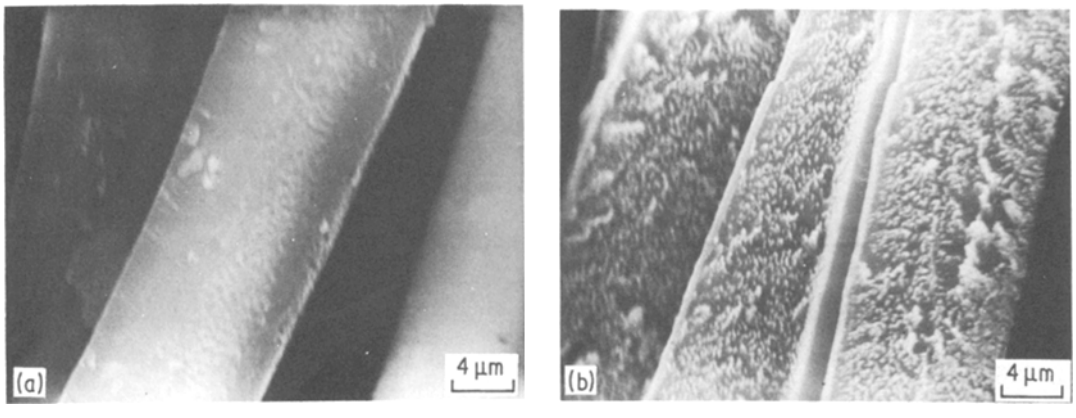

Figure 11 SEM photomicrographs of polyester fibres, (a) before ion irradiation, and (b) after natural texturing.

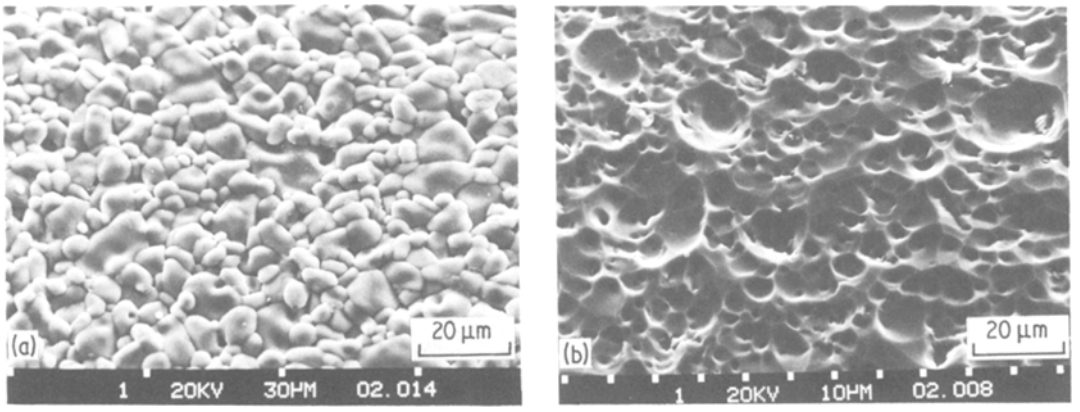

Figure 12 Scanning electron images of 96% alumina, (a) untreated surface, (b) surface after 90 min of ion-beam sputtering at an accelerating voltage of 7 kV. SEM performed in Laboratory of Electron Microscopy, Technical University of Wroclaw, Poland.

However, it is possible to alter the surface morphology by changing the beam incidence angle [167]. Three sets of SEM images presented below show the great influence of this parameter on the morphology and on potential possibility of surface texturing in a controlled manner. For example, surfaces of polycrystalline 99.9% titanium samples (an example of the untreated surface is shown in Fig. 8a) ion bombarded from a hollow anode gun at various ion beam incidence angles, from 0 to 1.4 rad, were drastically changed, as can be seen in Fig. 14. Different angles "gave" different images of texture. A lot of various topographical features could be observed: (a) flat and shallow craters, variously shaped hillocks and isolated areas with periodic structure on a normally sputtered surface (Fig. 14a), (b) craters, slots, steps, cone-like features and grooves or etch lines on surfaces irradiated on an average inclined beam (Figs. 14b and c), and (c) etch lines, ridges and extensive topographical features similar to the "scale-like" structure on surfaces bombarded by a strongly inclined beam (Figs. 14d and e). All topographical features observed on natural textured surfaces of titanium were oriented along the ion beam direction, as is distinctly visible for near-glancing beam incidence, i.e. for 1.22 and 1.4 rad. Similar results were obtained for alloy–biomaterial, i.e. for chrome–nickel stainless steel (Figs. 15a to d). Ion bombardment developed on initially smooth surfaces, as seen in Fig. 9a, a large number of topographical elements, such as: (a) pits, craters, steps, terraces or deep holes on perpendicularly sputtered sample (Fig. 15a), (b) deep and differently shaped craters, cones and cone-like structures, as well as waves and periodic structures (etch lines), all distinctly oriented along the tangential component of the ion beam, on the sample irradiated at angle of 0.78 rad, and (c) etch lines, grooves, ridges, and scale-like structures (also oriented along the beam direction) on the samples sputtered at near-glancing incidence (Figs. 15c and d).

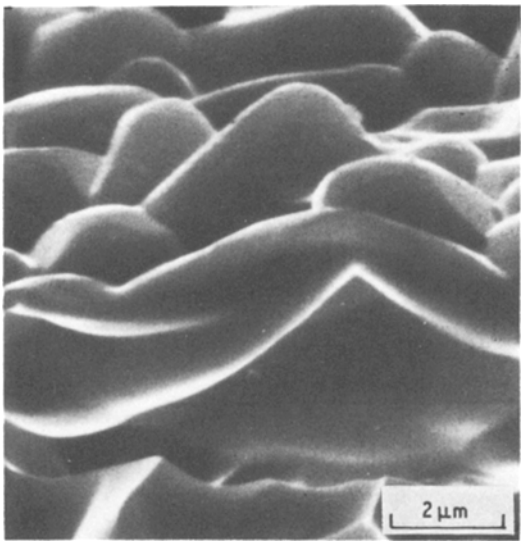

Figure 13 Border between the untreated (upper part) and natural textured (lower part) alumina surface obtained by Ar^+ ions irradiation from the hollow anode surface [60, 159]. SEM performed by W. Hauffe, Technical University of Dresden, GDR.

Two events are characteristic in natural texturing at various incidence angles ($NTex_{\Theta}$). Firstly, this technique develops different kinds of topographical features on different types of target

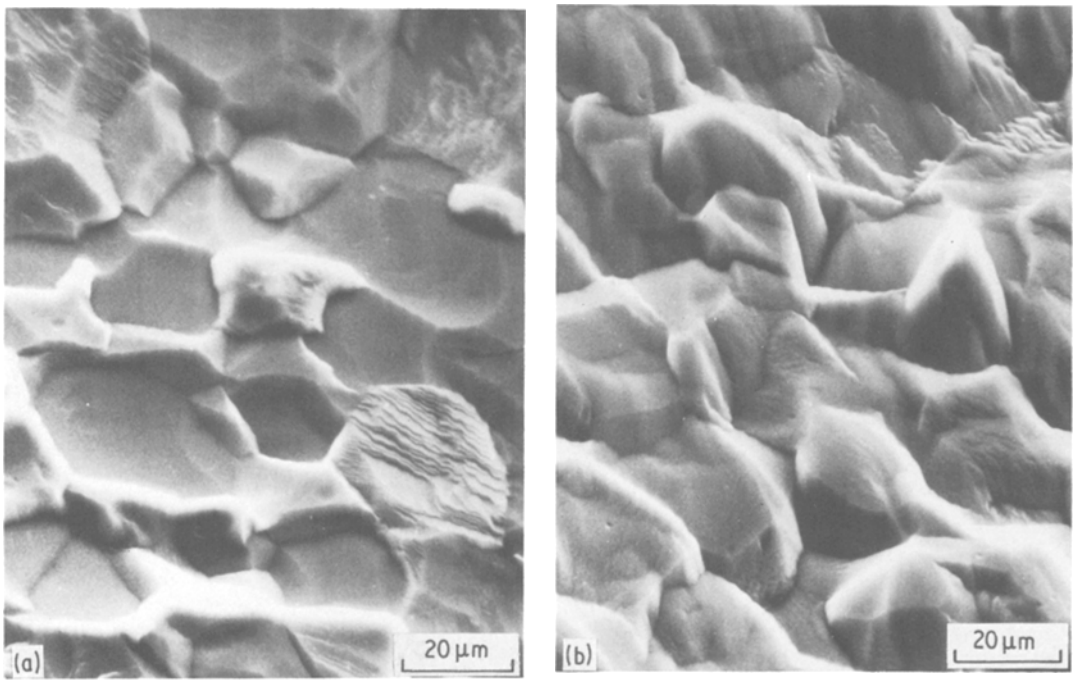

Figure 14 Titanium surface topography after natural texturing for 240 min at an accelerating voltage of 7 kV and at various incidence angles: (a) 0 rad, (b) 0.78 rad, (c) 1.05 rad, (d) 1.22 rad, (e) 1.4 rad.

materials but some of them are common. These common or similar shapes can be observed especially for very oblique beam incidence. Secondly, all developed features are oriented along the ion beam direction. This individual characteristic is independent of the type of material sputtered. Even such biocompatible material as alumina ceramic (which is an insulator and an extremely sputter-resistant material) was textured in the same manner and revealed analogical structures for near-glancing incidence (see Fig. 16). For these ion incidence angles, ion sputtering is dominated by collisions occurring in the first surface layers. Such behaviour is thought to be caused by a rapid increase in the reflection coefficient. With increasing incidence angle, Θ, the average path length travelled inside the target, and hence the energy loss, and hence sputtering yield, decreases. Fig. 17 shows the influence of the ion incidence angle Θ on the average path length (Fig. 17a) and on sputtering yield of alumina (Fig. 17b). It is difficult to say anything definite about the mechanism of formation of topographical features observed on all ion irradiated surfaces of biomaterials. However, this mechanism is a phenomenon located near the surface, it is more complicated because these first layers of polycrystalline biomaterials studied (for example alumina ceramic) were amorphized during ion beam bombardment. It has been suggested [168] that to explain the etch lines and scale-like topography one should take into consideration

Figure 14 Continued.

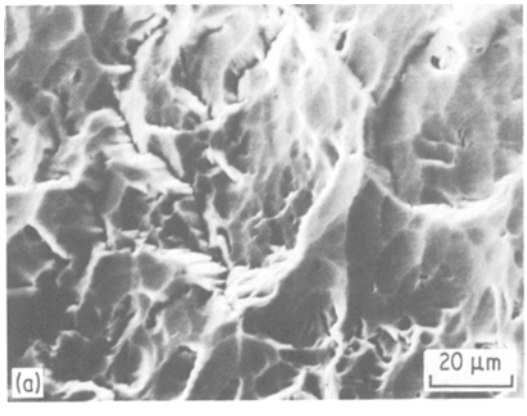

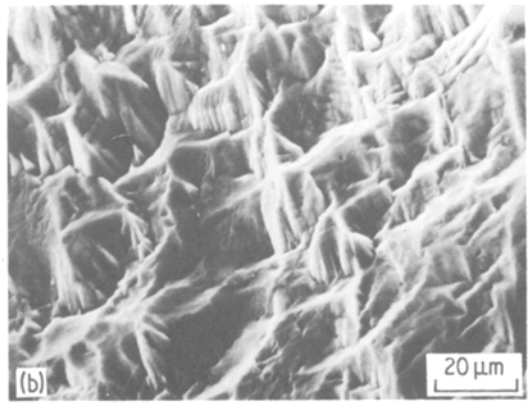

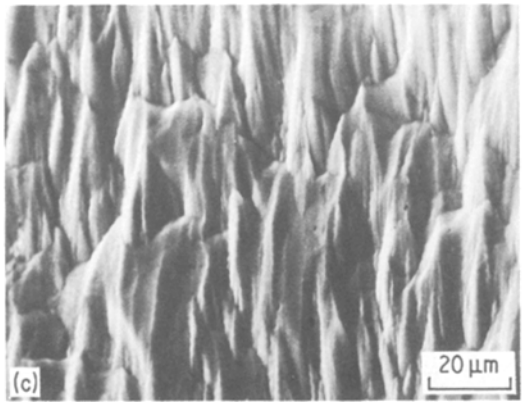

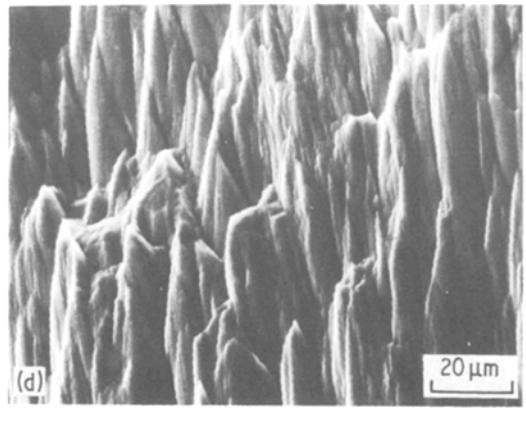

Figure 15 SEM images of natural textured surfaces of chrome–nickel stainless steel. Samples were ion bombarded for 240 min from a hollow anode gun (accelerating voltage of 7 kV) at various incidence angles from 0 to 1.22 rad, (a) 0 rad, (b) 0.78 rad, (c) 1.05 rad, (d) 1.22 rad.

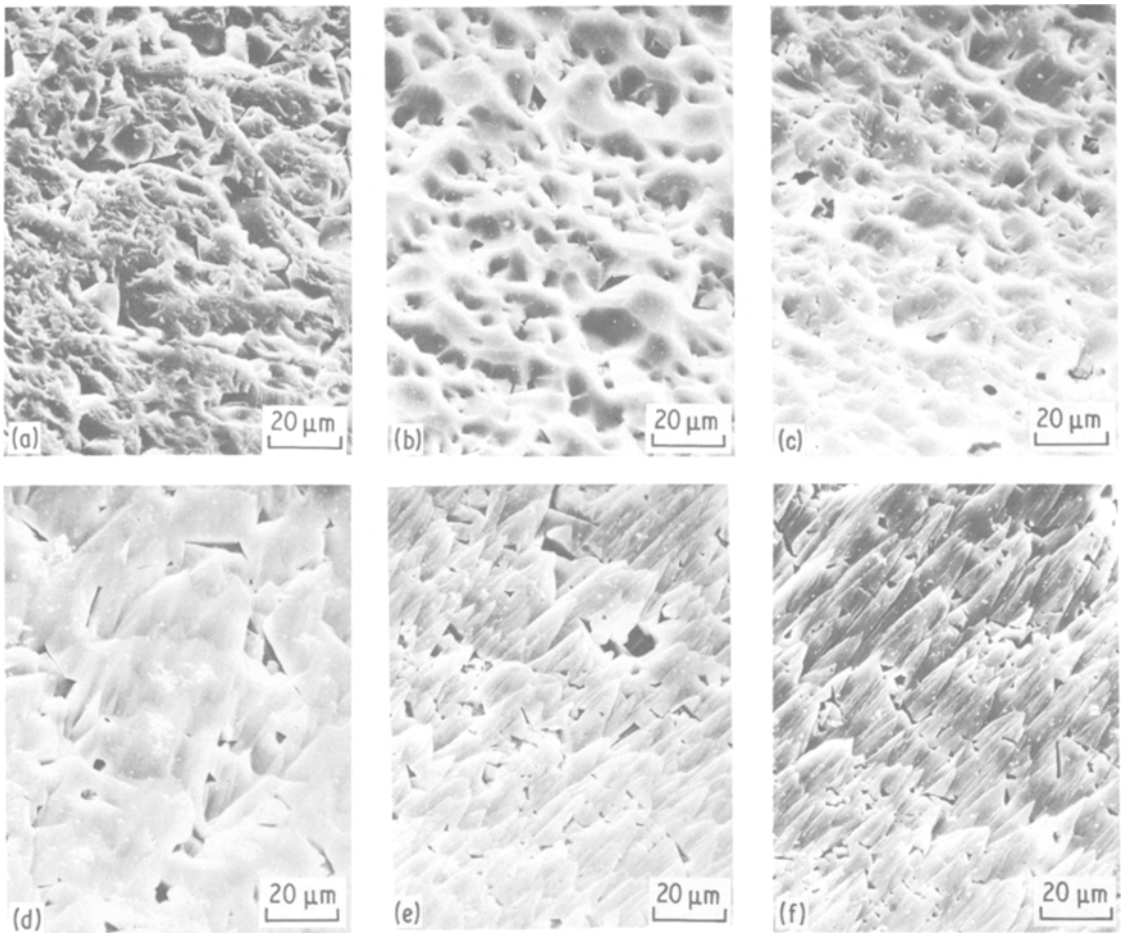

Figure 16 Surfaces of polycrystalline 99.5% alumina, (a) before, and after ion beam bombardment from a hollow anode source at an accelerating voltage of 7 kV and at various incident angles: (b) 0 rad, (c) 0.78 rad, (d) 1.05 rad, (e) 1.22 rad, (f) 1.4 rad.

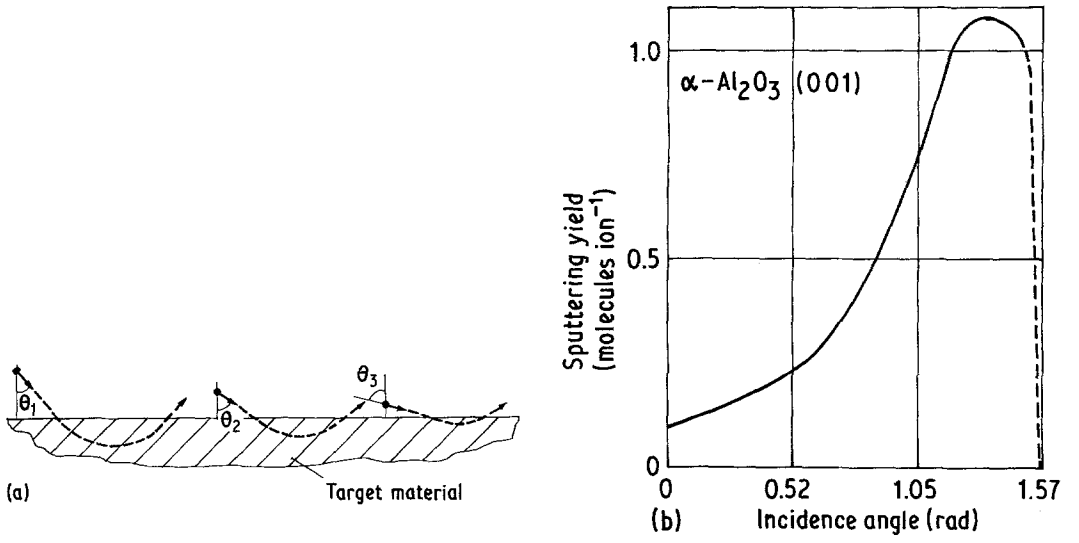

Figure 17 The influence of ion incidence angle Θ on: (a) average path length travelled inside the target $\Theta_1 \leqslant \Theta_2 \leqslant \Theta_3$, • Ion, and (b) sputtering yield (data from Holland *et al.* [1], p. 373).

TABLE VI Angular dependence of the K_{max}, K_{min}, and K_m coefficients for Ar^+ irradiation from hollow anode source of 99.5% alumina [167]

Beam incidence angle (rad)	0	0.78	1.05	1.22	1.4
Maximum coefficient, K_{max}	2.12	0.78	1.08	0.94	0.71
Minimum coefficient, K_{min}	0.97	0.74	0.69	0.66	0.59
Mean coefficient, K_m	1.29	0.76	0.88	0.79	0.65
Mean coefficient of selected samples (seen in Fig. 16)	1.17	0.76	0.69	0.68	0.60
Figure number	16b	16c	16d	16e	16f

the following:

1. the initial geometry of the sample surface, and
2. the strong dependence of sputtering yield on ion incidence angle.

In spite of the importance of the second event, the first one is rather controversial. The topographical features in question which developed on the surface after oblique ion beam irradiation have been observed not only on initially rough, but also on smooth surfaces.

In addition to the ion bombardment induced surface topography, modification of the surface roughness also can be observed and measured [163]. It is convenient to introduce a coefficient $K = R_A/R_B$, where R_A is the mean roughness after, and R_B before ion irradiation. This coefficient shows the changes of the roughness resulting from texturing of the target surface. Table VI describes the angular dependence of the maximum, minimum and mean coefficients for Ar^+ irradiation ($NTex_\Theta$) of 99.5% alumina samples as well as mean coefficients K_m of some specimens selected from all samples analysed. Surfaces of these selected specimens are presented in Fig. 16.

A substantial increase of surface roughness can be observed for perpendicular (near-perpendicular) bombardment. For very oblique ion incidence roughness is greatly reduced.

4.2.1.2. Seed texturing. Sputtering with a sputter-resistant material, seed material, supplying the target surface during ion irradiation is normally referred to as seed texturing (STex).

A low sputtering yield seed material (see Fig. 18a) is located in the proximity of the target and usually at a 0.52 to 0.78 rad angle with respect to the ion beam axis. The ion beam simultaneously sputters both, the target and the seed material. Some of the seed material is deposited on the target surface. It has been generally understood that the obtained surface texture results from clusters of seed atoms protecting the underlying substrate while the surrounding substrate material is sputtered away. It is possible to texture surfaces differently (Fig. 18b), i.e. using two separate processes [169] as: (a) deposition of seed material onto the target surface by means of, e.g. ion sputter deposition technique (ISD), and (b) ion sputter texturing of the target in question with a thin film of seed material covering its surface.

In analytical models of the dynamics of seed texturing [170, 171] seed atoms are assumed to move from adsorption site to adsorption site on the target surface by a random walk process. Only those atoms that acquire an energy greater than the activation energy E_d (i.e. the potential barrier between adjacent sites) are mobile. This energy ranges from 0.5 to 2.0 eV for metallic materials of interest for seeding. The radius r_d

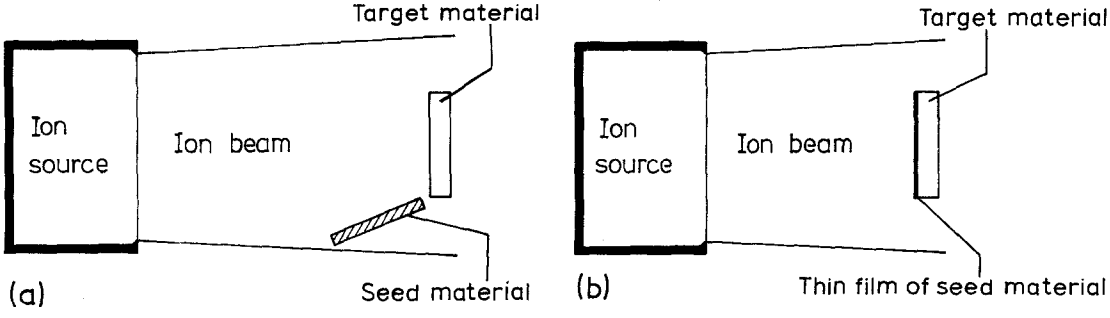

Figure 18 Schematic representation of seed texturing techniques (a) generally used, (b) applied occasionally.

TABLE VII Melting points and sputtering yields of various elements [154]

Symbol	Elements	Melting point, (°C)	Sputtering yield (at ion^{-1})	Symbol	Elements	Melting point, (°C)	Sputtering yield (at ion^{-1})
Ag	Silver	960.8	3.12	Ni	Nickel	1453.0	1.45
Al	Aluminium	660.0	1.05	Os	Osmium	3000.0	0.87
Au	Gold	1063.0	2.40	Pb	Lead	327.4	2.7
B	Boron	2030.0	–	Pd	Palladium	1552.0	2.08
Be	Berylium	–	0.51	Pt	Platinum	1769.0	1.40
Bi	Bismuth	271.3	–	Rb	Rubidium	–	1.15
C	Carbon	3727.0	0.12	Re	Rhenium	3180.0	0.87
Cd	Cadmium	320.9	–	Rh	Rhodium	1966.0	1.30
Co	Cobalt	1495.0	1.22	Ru	Ruthenium	2500.0	–
Cr	Chromium	1875.0	1.18	Sb	Antimony	630.5	–
Cu	Copper	1083.0	2.35	Si	Silicon	1410.0	0.50
Dy	Dysprosium	–	0.88	Sm	Samarium	–	0.80
Er	Erbium	–	0.77	Sn	Tin	231.9	–
Fe	Iron	1536.0	1.10	Ta	Tantalum	2996.0	0.57
Ga	Gallium	29.8	–	Th	Thorium	–	0.62
Gd	Gadolinium	–	0.83	Ti	Titanium	1668.0	0.51
Ge	Germanium	937.4	1.1	U	Uranium	–	0.85
Hf	Hafnium	2222.0	0.70	V	Vanadium	1900.0	0.65
In	Indium	156.2	–	W	Tungsten	3410.0	0.57
Ir	Iridium	2454.0	1.01	Y	Yttrium	–	0.68
Mn	Manganese	1245.0	–	Zn	Zinc	419.5	–
Mo	Molybdenum	2610.0	0.80	Zr	Zirconium	1852.0	0.65
Nb	Niobium	2468.0	0.60				

– No data

over which surface diffusion can be expected to take place is given by the expression:

$$r_d = 2 \times 10^{-4} \exp(-E_d/2kT). \quad (4)$$

where T is substrate temperature. Having found the radius from which diffusion will supply a seed cluster, it is appropriate to consider its stability, because there is a critical size for a seed cluster below which steady growth is not possible. This stability will depend on the diffusion rate to the cluster being sufficient or insufficient to supply the sputtering loss from a cluster of critical radius. The required diffusion radius r_d to sustain a cluster of critical radius r_c is:

$$r_d = r_c/F_s^{1/2}, \quad (5)$$

where F_s is the ratio of incident seed atoms to incident ions.

A seed texturing theory [170, 171] accurately predicts a mimimum critical temperature for texturing:

$$T = 587 E_d, \quad (6)$$

where E_d is in eV. The existence of the minimum temperature in question is also important for the production of smooth surfaces, in that a sufficient reduction in surface temperature should reduce the mobility of any seed material enough to avoid texturing (conning).

The seed material sputtering yield does not always have to be lower than the target material in order that texturing occurs [53, 150, 170–172]. Firstly, it was predicted from the theory, and also verified experimentally, that a high sputter yield material could serve as a seed for texturing of a lower sputter yield material if the seed were sufficiently mobile on the target surface. Secondly, it seems that the seed material must simply have a higher melting temperature than the target material to be textured. Melting points of various elements as well as sputtering yields of different targets are listed in Table VII.

The seed texturing technique occasionally called impurity-induced texturing [172], using various seeds was attempted on different target materials [53, 169, 173]. Among them biomaterial targets and/or biocompatible materials were successfully textured [156, 158, 159, 174]. Their surface morphologies were unique. A large number of topographical features or morphological structures could be observed but, generally, two main types were predominant: a ridge and a cone-like structure (texture). Many of the biocompatible materials had morphologies that

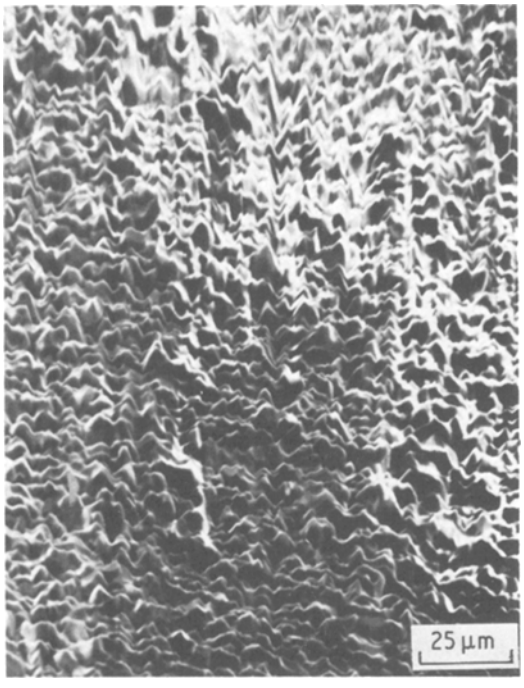

Figure 19 SEM image of a tungsten seed textured 96% alumina surface with a thin film of seed material deposited by means of the ISD technique prior to the ion texturing process (also see Fig. 18b). Ion irradiation was performed using a hollow anode gun for 90 min at an accelerating voltage of 7 kV, and with a small ion dose.

looked like densely packed cones, needles or "blunt grass-like stalks" [150].

Fig. 19 is the SEM photomicrograph of the 96% alumina surface after ion beam texturing with tungsten seed. Prior to the sputtering process the seed material was deposited by means of an ion sputter deposition technique (ISD) in a DC triode sputtering system (see Fig. 18b). Densely packed cones or cone-like structures were the prevailing features developed during ion beam bombardment. This image of the alumina surface morphology is rather unique, probably owing to the relatively small beam current density. It is worth noting, that in the absence of heating, even in the presence of a seed material, only short-lived cones develop which are soon completely eroded [172]. This is clearly seen in Figs. 20a and b, where cone or ridge like texture cannot be observed on the presented alumina surfaces, independent of the seed texturing technique used in the experiment. On the first surface, which was seed textured according to Fig. 18a, only isolated cones can be found. The next surface topography obtained after ion bombardment of the surface covered with a thin film of seed material, is similar to that obtained by natural

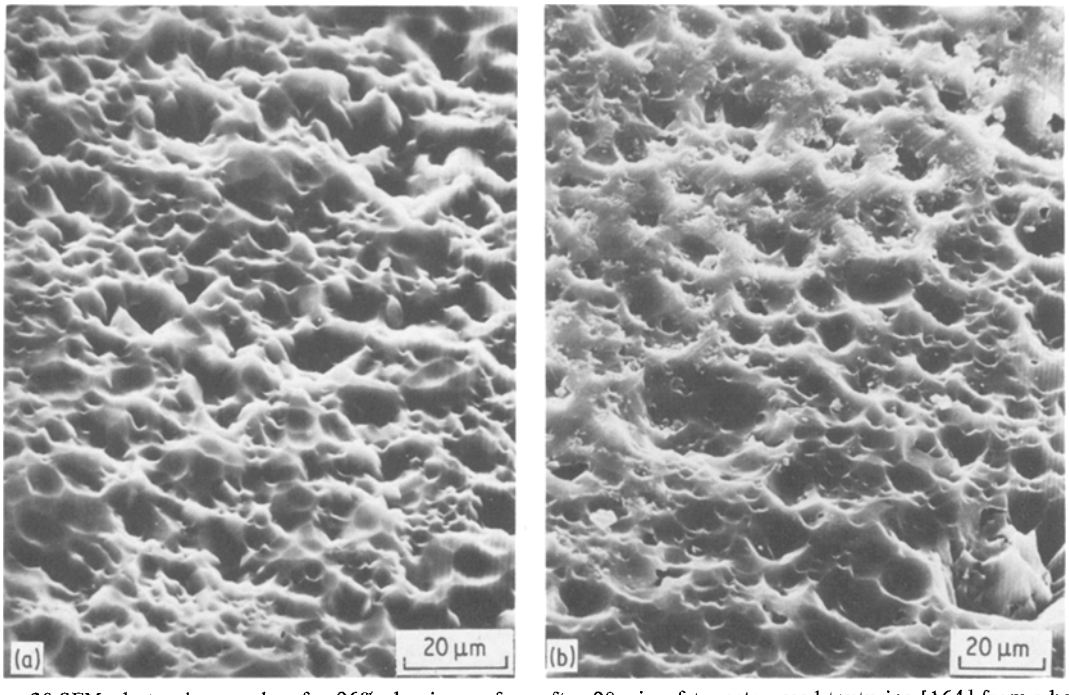

Figure 20 SEM photomicrographs of a 96% alumina surface after 90 min of tungsten seed texturing [164] from a hollow anode gun at an accelerating voltage of 7 kV, and with a maximum beam current density (large ion dose), (a) by means of an external seed material plate (see Fig. 18a), and (b) using a thin film of seed material covering the target surface prior texturing (see Fig. 18b).

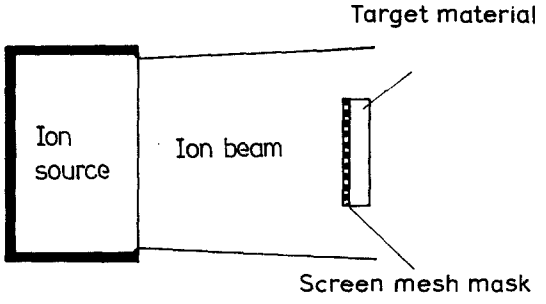

Figure 21 Schematic representation of pattern texturing.

texturing (see Fig. 12b). The only important difference is the presence of surface inclusions from the sputtered thin film of tungsten seed.

4.2.1.3. Pattern texturing. The third way of sputter texturing of a solid surface, shown in Fig. 21, is ion sputtering through a screen mesh mask imposed on the material during ion irradiation. The screen prevents the erosion of the target material directly beneath it, resulting in the surface with an array of pores of constant dimension, for example the square hole pattern etched in the surface. The technique is referred [154] to as pattern texturing (PTex). Different surface pore (or pit) shapes and dimensions can be obtained by varying the shape and the size of the screen apertures as well as the ion texturing duration (properly the ion dose). To ensure the precise projection of the apertures onto the sputtered target surface it is important to hold the screen in intimate contact with the target and to make the mesh of sputter resistant material. The sputtering yield of the screen mesh relative to the target material determines the maximum depth to which the pits (or pores) can be sputtered prior to complete sputter loss of the mesh [150]. It means that the higher the sputter yield of the target material the deeper the pores can be etched.

The pattern texturing technique gives the possibility of controlled and precise texturing of biocompatible materials. By using screen masks (e.g. with various apertures between 20 and 150 μm [157]), surfaces with uniform macrostructure can be obtained (see Fig. 22). Contrary to these rather optimistic results, the surface microstructure observed at the bottom of individual pits is not so uniform and differs from pit to pit. These differences are much more pronounced if one compares several pits selected from various pattern textured biocompatible materials (see Fig. 23). The unique microstructure developed at the bottom of each pit depends on many factors. Among them target material properties, the etch rate of the screen mesh relative to the target material, and sputtering conditions (e.g. rate of ion beam neutralization) are probably the most important. The microstructure in question is usually similar to that obtained after natural texturing (compare for example Figs. 8b and 9c), particularly when the same sputtering conditions were used. In the case of non-conductors, pattern textured with a not fully neutralized ion beam, irregular sputtering of the pit due to the local repulsion and distortion of the beam is possible. The resulting surface topography (see Fig. 23c) of pit bottom is also irregular: different features in its central region and in the vicinity of the mesh mask (cones or cone like features) as well as deeper etching of the pit near the screen mesh can be observed. These two events are induced by the existence of a usually high sputter resistant mesh mask, which is a source of: (a) seed atoms supplying the pattern textured surface with low sputtering yield atoms, and (b) electrons (properly, secondary electrons) preventing the surface charging. It is self-evident that the events in question must also be considered in pattern texturing of conductive materials.

It may be appropriate at this point to mention that associated with both, seed and pattern texturing techniques, there is some contamination of the target material with the seed and mesh material. This can be partially removed by further ion bombardment of the target after removing the seed plate or screen mesh mask but, unfortunately, this process can also alter the previously developed surface texture. Aqua regia acid bathing appears to eliminate much of these unwanted materials but small fractions usually remain entrapped [150]. It seems that the best way to minimize the contamination effect is to use the natural texturing technique or to apply transfer cast biomaterials peeled from pattern textured surfaces.

4.2.2. Related problems

4.2.2.1. Surface compositional changes. Processes and models relating to chemical composition changes induced by ion sputtering of solids were discussed earlier (in Section 3.2). It may be convenient to present here the practical aspects of the process which are very important, especially in the field of biomedical application of ion

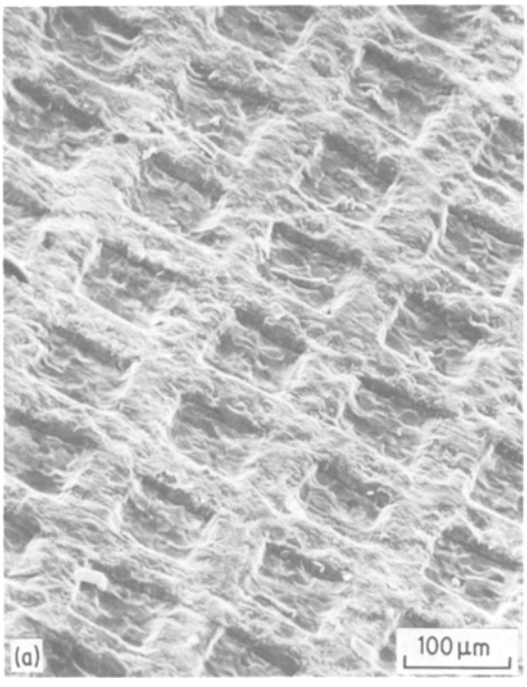

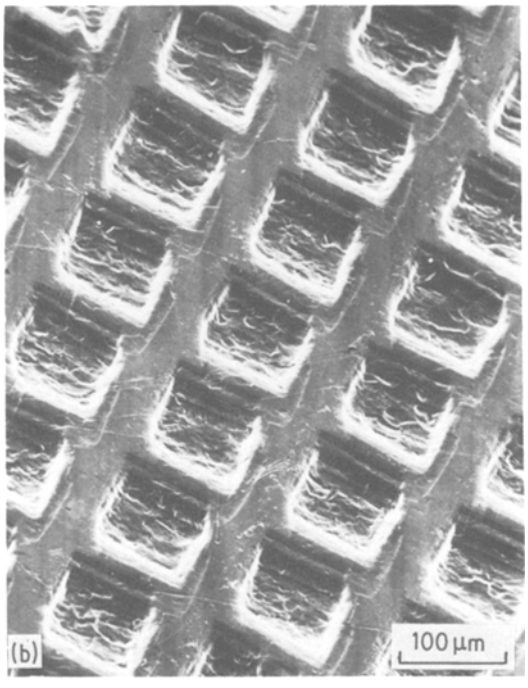

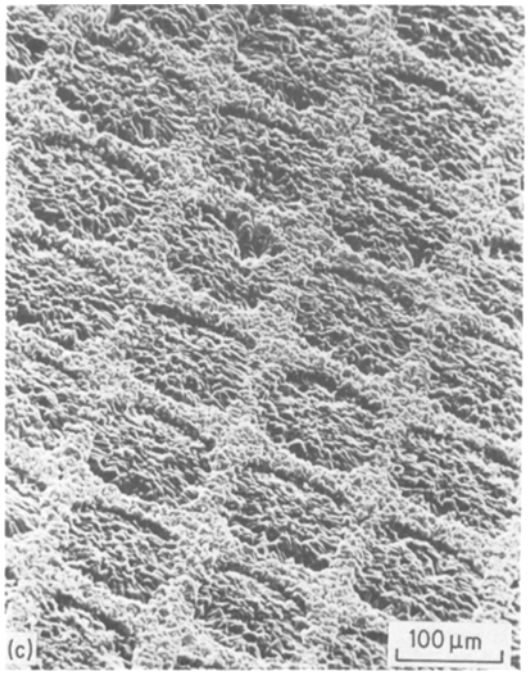

Figure 22 Pitted surfaces of three different materials presently used or under consideration for implant devices resulting from 210 min of pattern texturing [160] through the stainless steel screen mesh mask from a Kaufman-type source (1000 V, 2 mA cm^{-2}), (a) titanium, (b) chrome–nickel stainless steel, and (c) alumina. The depths of pits for each material depend on the etch rates and are proportional to the results obtained elsewhere and listed in Table V.

sputtering. Among them problems such as: the influence of ion sputtering on compositional changes of biocompatible materials as well as biomaterials, the question of whether these changes are significant or not, do they or do they not influence the mechanical properties of the materials in question and/or tissue response for the biomaterial after implantation, must be considered and experimentally verified. In the last decade some experiments were performed to investigate the influence of ion sputtering of biocompatible materials and biomaterials on their surface chemical composition. For example, ESCA results have shown that argon ion bombardment of iron–nickel–chromium and binary iron–nickel alloys (see reference [95] and Table IV) does not result in a significant alteration, about 10%, of the surface composition of either alloy. Also EDS (energy dispersion spectrometry) studies [174] indicated very little chemical change of the cobalt–chromium–tungsten surgical implant alloy. Except for biomedical alloys, the near-surface compositional changes of biocompatible polymers resulting from ion beam irradiation and based on ESCA and ISS were also investigated [150, 157, 175–177]. These materials included: polyurethanes, polyetherurethane, ultra-high molecular weight (UHMW) polyethylenes,

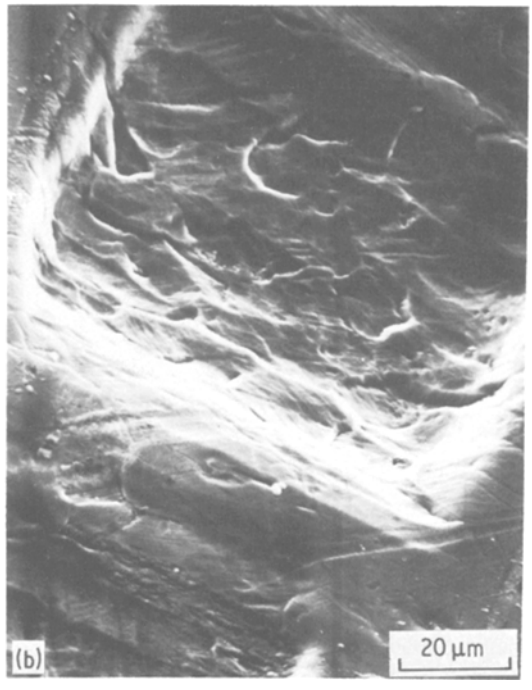

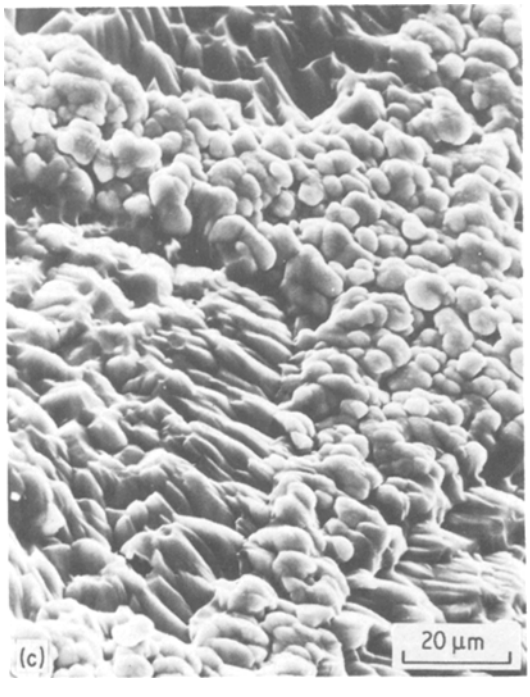

Figure 23 Isolated pits selected from the pattern textured surfaces presented in Fig. 21, [159]: (a) titanium, (b) chrome–nickel stainless steel, and (c) alumina.

polytetrafluoroethylene, polyoxymethylene, 2-hydroxyethylmethacrylate, and silicon rubber.

Naturally, it is too early to make any general conclusions with the few experimental results available so far. However, it can be said that the surface chemical changes of biocompatible materials (biomaterials) resulting from ion sputtering are rather minimal in spite of the often significant changes in the surface morphology (or texture).

Other interesting problems mentioned above, as for instance, the influence of compositional changes on mechanical properties or tissue response have not been solved up yet. The main difficulty is to distinguish the modification in mechanical properties and tissue response resulting from chemical alteration from that obtained due to morphological changes. It seems that additional studies are necessary.

4.2.2.2. Modification of mechanical properties. Information about the influence of ion beam sputtering on the mechanical properties of biocompatible materials (or biomaterials) is rather sparse [154]. There are only a few articles concerning this problem. In order to show the importance of the question, some experimental results, as examples, are presented below.

Several mechanical parameters, such as: ultimate strength [157, 174, 179], yield and fatigue strengths [157, 178, 179], ultimate tensile strength [175], strength of the bond between two different materials [174], hardness [174, 179],

and ductility [174] have been taken into consideration and measured. The ultimate strength and/or hardness of the cobalt–chromium–tungsten alloy (Haynes 25) and stainless steel were not reduced after the ion beam texturing process. Also the strength of the bond between polymethyl methacrylate and titanium–aluminium–vanadium alloy (Ti-6,4) was not significantly increased. The total elongations of the ion treated samples of Haynes 25 and stainless steel did not change from the control sample values, which indicates that ion sputtering does not modify the ductility of these materials. Standard diameter tensile samples of Haynes 25 and stainless steel, and standard fatigue samples of Ti-6,4 alloy and stainless steel were also sputtered to study the influence of ion processing on the mechanical properties. Examination of the effects of the ion textured surface on the ultimate, yield, and fatigue strengths revealed very little degradation of the properties. The results of the tensile tests for several biomedical polymers indicated a percent reduction in the ultimate tensile strength resulting from ion bombardment ranging from 1 to 19%. The general shape of the stress–strain curves for both, untreated and textured samples was the same. Very interesting fatigue tests were conducted at room temperature with test sections of a cobalt–nickel–chromium–molybdenum alloy (MP35N), as the fatigue specimens, immersed in an artificial physiological solution formulated to simulate the corrosive environment of the human body. Both types of surface texture, i.e. natural texture and square hole pattern texture, were found to reduce the fatigue strength below that of the smooth surface (for example, at 5×10^6 cycles the estimated factor of natural and pattern textured were reduced by approximately 50 to 60%).

Concluding this short section, it could be stated that the examination of the effects of an ion textured surface on the mechanical properties of representative biocompatible materials and/or biological implant materials revealed rather small changes in these properties.

5. Clinical implication and potential applications

So-called "biomedical applications of ion sputtering", relating to: (a) revealing the internal structure of biological derived materials, and (b) more intensively studied modification of surface texture of biocompatible materials (and/or biomaterials), give a great amount of potential clinical use. Of course, all new ideas, and new and even exciting applications must be experimentally verified on animals. This is the first step on the way to the clinical applications of every new conception. Preliminary findings as well as interesting examples of potential clinical use of ion beam textured biomaterials are presented and discussed below.

These problems which concern the revealing of the internal structure of biologically derived materials were discussed earlier and, therefore, they are beyond the scope of this section.

5.1. Main problems and preliminary findings

It can be generally accepted that, among other factors which affect the so-called biological tissue response to biomaterial, surface morphology is one of the most important. In order to develop clinically acceptable materials (biocompatible materials), the influence of their surface morphology on biological response must be understood. Different problems, such as, for example:

1. changes in the healing process that result from the presence of the sputtered implant, prosthesis or artificial organ,
2. a tissue inflammatory and/or foreign body response in the tissue surrounding the ion textured biocompatible material,
3. a firm attachment of the surrounding tissue or thrombus to the ion treated biomaterial used in the experiment,
4. the influence of surface texture of the biomaterial on the soft tissue or cell attachment kinetics,
5. the influence of surface morphology of various elements of assist devices on cell or tissue attachment, tissue inflammatory, etc. must be considered, depending on whether biomaterial is used in soft or hard tissue, in contact with the blood or other body fluids. Preliminary tissue response data have been obtained and described in the literature. Several important and interesting examples are discussed below.

The experimental results indicated a minimal tissue inflammatory or foreign body response and a close adaptation of interfacial tissue with the xenon ion textured titanium and cobalt–nickel–chromium–molybdenum (MP35N) dental implants, which were tested in beagles [157]. Also

canine tests have been performed to evaluate zirconia coated cobalt–chromium–molybdenum dental implants in which the surface was either smooth or pattern textured. The implant test periods ranged from 6 weeks to 1 year. The results of clinical evaluation of the performance of these biomaterials showed success to failure ratios of 0.6 for the textured and a 2.3 ratio for the smooth surface implants. The increased failure rate of the pitted surface materials can be characterized by gross mobility, inflammation, hyperplasia, etc. [150]. Natural textured MP35N, tantalum seed textured pure titanium and pattern textured aluminium oxide have also been studied as canine dental implants. Experimental results indicated no statistically significant differences in the clinical performance or mechanical retention of the implants and prevented any statistically significant conclusions as to whether a closer simulation of cementum morphology resulted in an improved dental implant performance. Recently it appeared that a greater emphasis must be placed on the examination of the textured surfaces of implants at the gingival percutaneous location rather than at the osseous level [150] (some fraction of dental implant failures occurred as a consequence of peridental disease resulting from an ineffective percutaneous seal rather than problems associated with the anchorage in bone).

Animal tests have shown that osseous tissue grew into the recesses formed on orthopaedic implant (or prosthesis) surfaces by ion texturing. Furthermore, the bonding and fixation properties of the prosthesis were enhanced (e.g. in comparison with smooth implants, the forces up to 18 times greater were required to push out the ion textured implants placed in dog tibia [178]). On the other hand, results of ion textured stainless steel, Ti-6,4, cobalt–chromium–molybdenum and MP35N alloys, which were implanted in the cortex of canine femurs, showed no statistically significantly difference between textured and smooth (untreated) implant shear strengths.

Concluding this short part of the results which concern the ion textured hard tissue implants, it can be stated that the ion processing of these materials influences the tissue response and mechanical retention of these materials differently. Usually this effect is profitable, sometimes no statistically relevant differences of the experimental results of sputtered and unsputtered samples can be observed, and finally, there are some exceptions where the process in question is unfavourable. It seems that the application of the ion textured hard tissue biomaterials will require the additional knowledge of the short and long term consequences.

The results of experiments relating to so-called soft tissue biomaterials (implants, prostheses, artificial organs, assist devices, etc.) are probably more optimistic. Pattern textured flat implants of PTFE, alumina, Haynes 25, Ti-6,4 and 316 stainless steel, which were implanted for 6 weeks in the dorsal subcutaneous soft tissue of rats and then investigated for mechanical attachment by means of a "pull out" test [157], revealed an increase in the tissue attachment to sputtered samples compared to untreated materials. There was also no evidence of an inflammatory cell response in the tissue surrounding the implants. Significant differences in the blood response have been found between the ion sputtered and untreated cardiovascular implants of segmented polyurethane which were implanted against the inside walls of canine femoral and carotid arteries [149]. Although the final thrombus thickness (after 4 days of implantation) was the same for both ion sputtered and unsputtered samples, the initial thrombus growth (after 1 day of implantation) was accelerated when compared to the growth on untreated samples. Interesting studies [150] carried out on ion textured and unsputtered PTFE and polyoxymethylene (Delrin) biomaterials, which were implanted into the intercostal musculature of rats have shown that ion processing induced the following modifications in the mononuclear phagocytes adjacent to the implant surface: increased cell adhesion, metabolism, acid phosphatase activity and increased foreign body giant cell formation. Also results of experiments with exudate extracted from within hollow crylindrical subcutaneous implants having smooth and natural textured surfaces indicated increased cell growth activity for exudate extracted from textured implants within approximately the first week of implantation. Similar results have been obtained for smooth, ion beam polished, natural textured, and pattern textured samples of PTFE [177], which were implanted in the peritoneal cavity of rats for periods ranging from 30 min to 14 day. In general the smooth surfaces attracted less cells than ion beam treated – ion sputtering increased the cell attachment by an order of

magnitude over the smooth (i.e. untreated or ion polished) surface of PTFE. The ion processing was observed to enhance not only cell attachment but also multinucleated giant cell to cell contact, and fibrous capsule formation.

The ability to enhance cell attachment to the surface of biocompatible materials is a very important feature of the ion texturing process. The results of experiments suggest that the avid adherence of cells to the surface texture could be used to extract them from body fluids in either diseased states such as leukemia or the routine removal in the separation from plasma. Gradations in texture, obtained by natural, seed or pattern texturing, could also be utilized to evaluate diseased states characterized by the lack of adherence to the surface [177]. It seems that this new area of clinical applications of ion beam texturing of biocompatible materials is very promising and important. Therefore further studies that investigate for example cell interactions with materials of different morphologies, the influence of surface texture on attachment kinetics [177], the problem of quantitative measurements of adhesion forces between different solid substrates for investigation of surface and interfacial properties of biomaterials [180], etc., are necessary.

5.2. Some examples of potential clinical use

A great variety of experiments have proved that ion texturing of biomaterials can give a potential possibility of practical clinical applications. One of the most promising fields is implantology. There are, of course, a lot of problems resulting from ion texturing of biomaterials prior to implantation. These which are common and characteristic for all types of the materials in question were presented in section 5.1. Those which are characteristic of the individual biomaterials, and especially: (a) the main purpose of ion texturing of each type of biomaterial (i.e. for example dental implant, artificial bone, left ventricular assist device, etc.), and (b) the resulting questions which must be considered and investigated, are quoted below together with selected examples of potential clinical use of the ion textured biomaterials [149, 150, 177].

5.2.1. Orthopaedic implants (prostheses, artificial bones or joins)

1. The main purpose of ion texturing: to provide orthopaedic fixation without the use of the usually applied polymethylmethacrylate bone cement which is the most important cause of failure.

2. Resulting questions to be considered: changes (possible reduction) in mechanical properties of textured implants, time of patient immobilization required for adequate bone ingrowth.

5.2.2. Dental implants

1. The main purpose of ion texturing: to secure a firm mechanical anchorage to a bone and satisfactory biological response to the implant at a bone–implant interface and gingival tissue–implant interface.

2. Resulting questions to be considered: identification of the morphological requirements to produce an effective percutaneous seal at the site of gingival penetration, reduction of the tendency for epithelial cell downgrowth.

5.2.3. Blood contacting biomaterials

5.2.3.1. Vascular prostheses

1. Main purpose of ion texturing: generation of a viable layer of endothelial cells covering the implanted and ion textured material.

2. Resulting questions to be considered: prevention of embolization (detachement of all or a portion of the thrombus) or/and occlusion (blockage) of the vascular prosthesis, discrimination between blood response due to relatively significant morphological as opposed to relatively small chemical surface alteration.

5.2.3.2. Artificial heart pump diaphragms

1. Main purpose of ion texturing: to secure a free of thrombus surface for the pump diaphragm or a strong adherence of the thrombus to the diaphragm surface without losing the high flex capabilities.

2. Resulting questions to be considered; similar to those described for vascular prostheses.

5.2.3.3. Left ventricular assist devices

1. Main purpose of ion texturing: to minimize neointima thickness and to secure its good attachment to the blood contacting surface of an implantable blood pump bladder material, to reduce the probability of embolic complications.

2. Resulting questions to be considered: similar to those described for vascular prostheses.

5.2.4. Power packs for pacemakers

1. Main purpose of ion texturing: to improve the mechanical adherence of the tissue to the surface of the power pack in order to protect it from reorientation or displacement in the surrounding tissue.

2. Resulting questions to be considered: evaluation of the biocompatibility of the textured surface, effectiveness of texturing in improving the adherence.

5.2.5. Percutaneous connectors

1. Main purpose of ion texturing: to assure an effective seal of the skin–percutaneous connector interface to prevent infection.

2. Resulting questions to be considered: the loss of a body fluid seal resulting from epidermal cell ingress and growth along the implant–tissue interface.

5.2.6. Cell attachment testers

1. Main purpose of ion texturing: evaluation of diseased states characterized by the lack of adherence of cells to the definite texture of the tester.

2. Resulting questions to be considered: the influence of surface texture on cell attachment kinetics, cell interactions with materials of different texture.

Numerous clinical applications of the technique in question have been identified and/or are now in various stages of experimental evaluation. It seems, that it is not possible to present all of them because the material is too extensive to be placed here. Therefore, at the end of this section only a few selected, but rather interesting and promising potential applications, as examples, are given, i.e.:

1. the application of defined surface texture and material for the peritoneal shunted hydrocephalic and peritoneal dialysis,

2. the use of transfer cast biopolymers peeled from pattern textured surfaces as blood contacting surfaces,

3. the research for an optimal transfer cast pillar texture to utilize it in the design of functional percutaneous connector devices,

4. the feasibility of using ion beam sputter ventilated microtubules to shunt cerebrospinal fluid directly from the ventricals upward to the subarachnoid space,

5. the possibility of application of an artificial ureter and a colostomy device, etc.

6. Conclusions

The unique capabilities of ion sputtering give chances of so-called biomedical applictions of the process. Two branches of the biomedical use seem to be particularly promising, i.e. revealing of the internal structure of biologically derived materials and the modification of the surface texture of biomaterials and/or biocompatible materials. Two different types of sputtering (i.e. sputter etching and sputter texturing) utilized in each branch result in various mechanisms and events which must be considered and understood.

In the last two decades a growing interest in the study of biomedical applications of ion sputtering could be observed. A number of experiments have been performed and numerous interesting results have been published up to now. In the first decade the dominant effort in the research was spent in the revealing of the subsurface features of biologically derived materials. Recently, the sputtering technique has become widely used in attempts to modify the surface texture of various biomaterials. It has been proved that ion sputtering is a valuable tool, not only in the examination of the internal structure of biological materials but also, and especially, in the surface texturing of biomaterials. These give practical possibility of potential clinical use. However, that is quite a problem!

The whole understanding and solving of biological and medical problems concerning biomedical and clinical applications of ion sputtering is not possible by ion beam users only. A large team of people working on biological, medical, and other related questions must give their experience in the field. Unfortunately, usually they are not aware of the existence of the technique in question.

It is the task of this paper to promote the ion beam sputtering technique among other research workers, and especially among biologists and medical doctors.

References

1. L. HOLLAND, W. STECKELMACHER and J. YARDWOOD (editors), "Vacuum Manual" (E and FN Spon, London, 1974) p. 370.
2. P. SIGMUND, in "Topics in Applied Physics", Vol. 1, edited by R. Behrish (Springer, Berlin, 1981) pp. 9–71.
3. G. BETZ and G. K. WEHNER, *ibid.* Vol. 2.
4. O. ALMEN and G. BRUCE, *Nucl. Instr. Methods* **11** (1961) 257.

5. N. LAEGREID and G. K. WEHNER, *J. Appl. Phys.* **32** (1961) 365.
6. D. ROSENBERG and G. K. WEHNER, *ibid.* **33** (1962) 1842.
7. K. B. CHENEY and E. T. PITKIN, *ibid.* **36** (1965) 3542.
8. H. M. WINDAWI, *Surf. Sci.* **55** (1976) 573.
9. E. P. VAULIN, N. E. GEORGEVA and T. P. MARTYNENKO, *Solid State Phys.* **19** (1977) 1423.
10. R. V. STUART and G. K. WEHNER, *J. Appl. Phys.* **33** (1962) 2345.
11. I. N. EVDOKIMOV and V. A. MOLCHANOV, *Can. J. Phys.* **46** (1968) 779.
12. P. SIGMUND, *Phys. Rev.* **184** (1969) 383.
13. H. H. ANDERSEN and H. L. BAY, *Radiat. Effects* **19** (1973) 139.
14. J. S. COLLIGON, C. M. HICKS and A. P. NEOKLEOUS, *ibid.* **18** (1973) 119.
15. E. S. MASHKOVA and V. A. MOLCHANOV, *ibid.* **18** (1973) 283.
16. H. H. ANDERSEN and H. L. BAY, *J. Appl. Phys.* **46** (1975) 2416.
17. E. P. EER NISSE, *Appl. Phys. Lett.* **29** (1976) 14.
18. M. J. WITCOMB, *Radiat. Effects* 27 (1976) 223.
19. *Idem, ibid.* **32** (1977) 205.
20. J. S. COLLIGON and M. H. PATEL, *ibid.* **32** (1977) 193.
21. F. VASILIU and S. FRUNZA, *Rev. Roum. Phys.* **22** (1977) 601.
22. Z. W. KOWALSKI, *J. Mater. Sci.* **16** (1981) 3512.
23. *Idem,* Polish Patent No. 121162 (1983).
24. Y. YAMAMURA, N. MATSUNAMI and N. ITOH, *Radiat. Effects* 71 (1983) 65.
25. Y. YAMAMURA, Proceedings of the Intenational Ion Engineering Congress – ISIAT'83 and IPAT'83, Kyoto 1983 p. 1875.
26. H. H. ANDERSEN and H. L. BAY, in "Topics in Applied Physics", Vol. 1, edited by R. Behrish (Springer, Berlin, 1981) pp. 145–218.
27. H. E. ROOSENDALL, *ibid.* pp. 219–256.
28. R. KELLY, *Radiat. Effects* **80** (1984) 273.
29. P. SIGMUND, *Rev. Roum. Phys.* **17** (1972) 823.
30. *Idem, ibid.* **17** (1972) 969.
31. *Idem, ibid.* **17** (1972) 1079.
32. *Idem, J. Mater Sci.* 8 (1973) 1545.
33. M. T. ROBINSON, in "Topics in Applied Physics", Vol. 1, edited by R. Behrish (Springer, Berlin, 1981) pp. 73–144.
34. M. J. NOBES, *Nucl. Instr. Methods* **170** (1980) 371.
35. G. CARTER, J. S. COLLIGON and M. J. NOBES, *Radiat. Effects* **31** (1977) 65.
36. A. R. BAYLY, *J. Mater. Sci.* 7 (1972) 404.
37. A. D. G. STEWARD and M. W. THOMPSON, *ibid.* 4 (1969) 56.
38. D. J. BARBER, F. C. FRANK, M. MOSS, J. W. STEEDS and I. S. T. TSONG, *ibid.* 8 (1973) 1030.
39. M. J. NOBES, J. S. COLLIGON and G. CARTER, *ibid.* **4** (1969) 730.
40. G. CARTER, J. S. COLLIGON and M. J. NOBES, *ibid.* **6** (1971) 115.
41. *Idem, ibid.* 8 (1973) 1473.
42. J. P. DUCOMMUN, M. CANTAGREL and M. MARCHAL, *ibid.* **9** (1974) 725.
43. J. P. DUCOMMUN, M. CANTAGREL and M. MOULIN, *ibid.* **10** (1975) 52.
44. N. HERMANNE and A. ART, *Radiat. Effects* 5 (1970) 203.
45. N. HERMANNE, *ibid.* **19** (1973) 161.
46. R. S. NELSON and D. J. MAZEY, *ibid.* **18** (1973) 127.
47. I. W. RANGEŁOW, *J. Vac. Sci. Technol.* **A1** (1983) 410.
48. S. M. ROSSNAGEL and R. S. ROBINSON, *ibid.* **1** (1983) 426.
49. I. H. WILSON, *Radiat. Effects* 18 (1973) 95.
50. A. R. BAYLY and P. D. TOWNSEND, *J. Phys. D: Appl. Phys.* **5** (1972) L103.
51. N. BIBIĆ, T. NENADOVIĆ, and B. PEROVIĆ, Proceedings of the 7th International Vacuum Congress, 3rd International Conference on Solid Surface, Vienna 1977, p. 1485.
52. R. S. DHARIWAL and R. K. FITCH, *J. Mater. Sci.* **12** (1977) 1225.
53. W. R. HUDSON, *J. Vac. Sci. Technol.* **14** (1977) 286.
54. J. L. WHITTON, *Radiat. Effects* 32 (1977) 129.
55. D. J. BARBER, *Beitr. Elektronenmikrosk. Dir. Oberfl.* **5** (1972) 585.
56. D. J. MAZEY, R. S. NELSON and P. A. THACKERY, *J. Mater. Sci.* **3** (1968) 26.
57. I. H. WILSON and M. W. KIDD, *ibid.* **6** (1971) 1362.
58. M. NAVEZ, C. SELLA and D. CHAPEROT, Colloques Internationaux CNRS, Bellevue, December, 1962, p. 233.
59. M. TARASEVICH, *Appl. Opt.* **9** (1970) 173.
60. M. LUKASZEWICZ and Z. W. KOWALSKI, *J. Mater. Sci.* **16** (1981) 302.
61. H. J. MATHIEU and D. LANDOLT, *Appl. Surf. Sci.* **3** (1979) 348.
62. T. KOSHIKAWA, K. GOTO, N. SAEKI, R. SHIMIZU and E. SUGATA, *Surf. Sci.* **79** (1979) 461.
63. P. S. HO, J. E. LEWIS and W. K. CHU, *ibid.* **85** (1979) 19.
64. G. BETZ, *ibid.* **92** (1980) 283.
65. R. KELLY, *ibid.* **100** (1980) 85.
66. G. BETZ, J. DUDONIS and P. BRAUN, *ibid.* **104** (1981) L185.
67. H. H. ANDERSEN, *J. Vac. Sci. Technol.* **16** (1979) 770.
68. J. E. LEWIS and P. S. HO, *ibid.* **16** (1979) 772.
69. H. G. TOMPKINS, *ibid.* **16** (1979) 778.
70. P. H. HOLLOWAY and G. C. NELSON, *ibid.* **16** (1979) 793.
71. P. SIGMUND, *ibid.* **17** (1980) 396.
72. G. BETZ, M. ARIAS and P. BRAUN, *Nucl. Instr. Methods* **170** (1980) 347.
73. G. BETZ, M. OPITZ and P. BRAUN, *ibid.* **182/183** (1981) 63.
74. G. K. WEHNER, *J. Vac. Sci. Technol.* **A1** (1983) 487.
75. Z. W. KOWALSKI, *ibid.* 1 (1983) 494.
76. A. A. PREDVODITELEV and N. V. OPEKUNOV, *Fiz. Chim. Obrabot. Mater.* **5** (1977) 44.
77. S. A. SCHWARZ and C. R. HELMS, *J. Vac. Sci.*

Technol. **16** (1979) 781.
78. J. DELAFOND, S. T. PICRAUX and J. A. KNAPP, *Appl. Phys. Lett.* **38** (1981) 237.
79. W. FARBER, G. BETZ and P. BRAUN, *Nucl. Instr. Methods* **132** (1976) 351.
80. P. S. HO, J. E. LEWIS and J. K. HOWARD, *J. Vac. Sci. Technol.* **14** (1977) 322.
81. H. J. MATHIEU and D. LANDOLT, *Surf. Sci.* **53** (1975) 228.
82. F. GARBASSI and G. PARRAVANO, *ibid.* **71** (1978) 42.
83. W. K. CHU, J. K. HOWARD and R. F. LEVER, *J. Appl. Phys.* **47** (1976) 4500.
84. A. JABLONSKI, S. H. OVERBURY and G. A. SOMORJAI, *Surf. Sci.* **65** (1977) 578.
85. P. S. HO, J. E. LEWIS, H. S. WILDMAN and J. K. HOWARD, *ibid.* **57** (1976) 393.
86. K. GOTO, T. KOSHIKAWA, K. ISHIKAWA and R. SHIMIZU, *J. Vac. Sci. Technol.* **15** (1978) 1695.
87. H. SHIMIZU, M. ONO and K. NAKAYAMA, *Surf. Sci.* **36** (1973) 817.
88. M. OPITZ, G. BETZ and P. BRAUN, Proceedings of the 4th International Conference on Solid Surface and 3rd European Conference on Surface Science, Cannes, 1980, p. 1225.
89. M. OPITZ, Thesis, University of Technology, Vienna (1979).
90. S. BERGLUND and G. A. SOMORJAI, *J. Chem. Phys.* **59** (1973) 5537.
91. F. J. KUJERS, B. M. TIEMAN and V. PONEC, *Surf. Sci.* **75** (1978) 657.
92. G. C. NELSON, *J. Vac. Sci. Technol.* **13** (1976) 974.
93. H. H. ANDERSEN, F. BESENBACHER and P. GODDIKSEN, Proceedings of the Symposium on Sputtering, Perchtoldsdorf, Vienna, 1980, p. 446.
94. Z. L. LIAU, W. L. BROWN, R. HOMER and J. M. POATE, *Appl. Phys. Lett.* **30** (1977) 626.
95. N. S. MCINTYRE and F. W. STANCHELL, *J. Vac. Sci. Technol.* **16** (1979) 798.
96. G. J. SLUSSER and N. WINOGRAD, *Surf. Sci.* **84** (1979) 211.
97. M. OPITZ, G. BETZ and P. BRAUN, *Acta Physica Acad. Sci. Hungarica* **49** (1980) 119.
98. S. H. OVERBURY and G. A. SOMORJAI, *J. Chem. Phys.* **66** (1977) 3181.
99. Y. TAGA and K. NAKAJIMA, *Trans. Jp. Inst. Met.* **18** (1977) 535.
100. A. VAN OOSTROM, *J. Vac. Sci. Technol.* **13** (1976) 224.
101. I. L. SINGER, J. S. MURDAY and L. R. COOPER, *ibid.* **15** (1978) 725.
102. G. E. McGUIRE, *Surf. Sci.* **76** (1978) 130.
103. R. BOUWMAN, L. H. TONEMAN and A. A. HOLSCHER, *ibid.* **35** (1973) 8.
104. M. MOHRI, K. WATANABE and T. YAMASHINA, *J. Nucl. Mater.* **75** (1978) 7.
105. G. K. WEHNER, "The Aspects of Sputtering in Surface Analysis Methods" in "Methods of Surface Analysis", edited by A. W. Czanderna (Elsevier, Amsterdam, Oxford, New York, 1975) Chap. 1, p. 5.
106. E. TAGLAUER and W. HEILAND, Proceedings of the Symposium on Sputtering, Perchtoldsdorf, Vienna (1980) p. 423.
107. C. C. CHANG, B. SCHWARTZ and S. P. MURARKA, *J. Electrochem. Soc.* **124** (1977) 922.
108. G. K. WEHNER, *Jpn. J. Appl. Phys. Suppl.* **2** (1974) 495.
109. H. C. FENG and J. M. CHEN, *J. Phys.* **C7** (1974) L75.
110. S. THOMAS, R. J. MATTOX, *J. Electrochem. Soc.* **124** (1977) 1942.
111. E. TAGLAUER and W. HEILAND, *Appl. Phys. Lett.* **33** (1978) 950.
112. H. J. MATHIEU, J. B. MATHEIU, D. E. McCLURE and D. LANDOLT, *J. Vac. Sci. Technol.* **14** (1977) 1023.
113. S. THOMAS, *Surf. Sci.* **55** (1976) 754.
114. K. JACOBI and W. RANKE, *J. Electron Spectrosc.* 8 (1976) 225.
115. K. S. KIM, W. E. BAITINGER, J. W. AMY and N. WINOGRAD, *J. Electron Spectrosc. Relat. Phenom.* **5** (1974) 351.
116. R. HOLM and S. STORP, *Appl. Phys.* **12** (1977) 101.
117. L. YIN, T. TSANG and I. ADLER, *Geochim. Cosmochim. Acta Suppl.* 7 (1976) 891.
118. T. J. CHUANG, C. R. BRUNDLE and K. WANDELT, *Thin Solid Films* **53** (1978) 19.
119. N. S. MCINTYRE and D. G. ZETARUK, *Anal. Chem.* **49** (1977) 1521.
120. T. J. CHUANG, C. R. BRUNDLE and D. W. RICE, *Surf. Sci.* **59** (1976) 413.
121. Y. UMEZAWA and C. N. REILLY, *Anal. Chem.* **50** (1978) 1290.
122. G. J. COYLE, T. TSANG, I. ADLER and L. YIN, *J. Electron Spectrosc. Relat. Phenom.* **16** (1979) 389.
123. N. S. MCINTYRE and D. G. ZETARUK, *J. Vac. Sci. Technol.* **14** (1977) 181.
124. T. TSANG, G. J. COYLE, I. ADLER and L. YIN, *J. Electron Spectrosc. Relat. Phenom.* **16** (1979) 389.
125. L. I. YIN, S. GHOSE and I. ADLER, *Appl. Spectrosc.* **26** (1972) 355.
126. C. R. BRUNDLE, T. J. CHUANG and K. WANDELT, *Surf. Sci.* **68** (1977) 459.
127. K. S. KIM and N. WINOGARD, *ibid.* **43** (1974) 625.
128. K. S. KIM, W. E. BAITINGER and N. WINOGRAD, *ibid.* **55** (1976) 285.
129. E. GÖRLICH, J. HABER, A. STOCH and J. STOCH, *J. Solid State Chem.* **33** (1980) 121.
130. G. C. NELSON, *J. Vac. Sci. Technol.* **15** (1978) 702.
131. A. KATRIB, *J. Electron Spectrosc. Relat. Phenom.* **18** (1980) 275.
132. J. ROTH, Proceedings on the Symposium on Sputtering, Perchtoldsdorf, Vienna (1980) p. 773.
133. J. ROTH, J. BOHDANSKY and A. P. MARTINELLI, *Radiat. Effects* 48 (1980) 213.
134. L. L. TONGSON, J. V. BIGGERS, G. O. DAYTON, J. M. BIND and B. E. KNOX, *J. Vac. Sci. Technol.* **15** (1978) 1133.
135. P. N. ROSS, J. R. and P. STONEHART, *J. Catal.* **39** (1975) 298.
136. A. TUROS, W. F. VAN DER WEG, D. SIGURD and J. W. MAYER, *J. Appl. Phys.* **45** (1974) 2777.

137. J. TARDY, J. PIVOT, J. P. DUPIN and A. CACHARD, Proceedings of the 7th International Vacuum Congress and 3rd Internation Conference on Solid Surfaces, Vienna, (1977) p. 1481.
138. J. L. WHITTON, G. SØRENSEN and J. S. WILLIAMS, *Nucl. Inst. Methods* **149** (1978) 743.
139. Z. L. LIAU and J. W. MAYER, *J. Vac. Sci. Technol.* **15** (1978) 1629.
140. J. M. POATE, W. L. BROWN, R. HOMER, W. M. AUGUSTYNIAK, J. W. MAYER, K. N. TU and W. F. VAN DER WEG, *Nucl. Instr. Methods* **132** (1976) 345.
141. Z. L. LIAU, J. W. MAYER, W. L. BROWN and J. M. POATE, *J. Appl. Phys.* **49** (1978) 5295.
142. D. K. MURTI, R. KELLY, Z. L. LIAU and J. M. POATE, *Surf. Sci.* **81** (1979) 571.
143. H. L. GARVIN, Symposium on Sputtering, Rochester, NY, 1969 p. 1.
144. P. R. STUART, J. S. OSBORN and S. M. LEWIS, *Vac.* **19** (1969) 503.
145. M. SPECTOR, L. C. BURNS and S. L. KIMZEY, *Nat.* **247** (1974) 61.
146. G. M. HODGES, M. D. MUIR, C. SELLA and A. J. P. CARTEAUD, *J. Microsc.* **95** (1972) 445.
147. I. BENDET and N. RIZK, *Biophys. J.* **16** (1976) 357.
148. S. N. GHAFOURI, R. K. FITCH and P. C. BALL, *Vac.* **31** (1981) 33.
149. B. A. BANKS, A. J. WEIGAND, CH. A. BABBUSH and C. L. VAN KAMPEN, NASA TM X-73512. (1976) p. 1.
150. B. A. BANKS, NASA TM 81721 (1981) p. 1.
151. Z. W. KOWALSKI, *Probl. Technol. Med.* **XII** (1981) 259.
152. *Idem, ibid.* **XIII** (1982) 47.
153. *Idem,* Scientific Papers IET Technical University of Wrocław No. 26, Monographs No. 9 (1982) 1.
154. *Idem, J. Mater. Sci.* **18** (1983) 2531.
155. Z. W. KOWALSKI, J. MARTAN and J. ZDANOWSKI, Reports of IET Technical University of Wrocław, Report No. 12/SPR, Wrocław, 1981.
156. A. J. WEIGAND and B. A. BANKS, *J. Vac. Sci. Technol.* **14** (1977) 326.
157. A. J. WEIGAND, NASA TM 78851 (1978) p. 1.
158. Z. W. KOWALSKI, *J. Mater. Sci.* **17** (1982) 2599.
159. Z. W. KOWALSKI and I. W. RANGELOW, *ibid.* **18** (1983) 741.
160. I. W. RANGELOW and Z. W. KOWALSKI, Beitr. elektronenmikrosk. Dir. Oberfl. **15** (1982) 27.
161. H. KATO, H. MIZUNO, K. TAMURA, S. WATANABE, Y. SHIMIZU, T. TERAMATSU, Y. KITAMURA and M. HIRABAYASHI, *Artif. Organs* **5** *Suppl.* (1981) 493.
162. H. KATO, T. NAKAMURA, H. MIZUNO, S. MATSUNOBE, K. TAMURA, S. WATANABE, Y. SHIMIZU and T. TERAMATSU, *Jpn. J. Artif. Organs* **11** (1982) 983.
163. Z. W. KOWALSKI, *J. Mater. Sci.* **17** (1982) 1627.
164. *Idem, Mater. Sci.* **VIII**, No. 1–4 (1982) 85.
165. *Idem,* "Ceramic Surfaces and Surface Treatments", edited by R. Morrell and M. G. Nicholas (British Ceramic Society, Stoke-on-Trent, 1984) pp. 77–87.
166. M. LUKASZEWICZ and W. HAUFFE, Scientific Papers IET Technical University of Wrocław No. 24, Conferences No. 4 (1980) p. 234.
167. Z. W. KOWALSKI, *J. Mater. Sci.* **19** (1984) 2845.
168. I. A. TEODORESCU and F. VASILIU, *Radiat. Effects* **15** (1972) 101.
169. W. R. HUDSON, R. R. ROBSON and J. S. SOVEY, NASA TM X-3517 (1977) p. 1.
170. R. S. ROBINSON, NASA CR-159567 (1979) p. 1.
171. H. R. KAUFMAN and R. S. ROBINSON, *J. Vac. Sci. Technol.* **16** (1979) 175.
172. R. S. ROBINSON and S. M. ROSSNAGEL, *ibid.* **21** (1982) 790.
173. R. S. BERG and G. J. KOMINIAK, *ibid.* **13** (1976) 403.
174. A. J. WEIGAND, M. L. MEYER and J. S. LING, NASA TM X-3553 (1977) p. 1.
175. A. J. WEIGAND and M. A. CENKUS, NASA TM–79245 (1979) p. 1.
176. D. W. DWIGHT and B. R. BECK, *Org. Coatings Plast. Prepr.* **40** (1979) 494.
177. G. J. PICHA, NASA CR 159817 (1980) p. 1.
178. E. G. WINTUCKY, M. CHRISTOPHER, E. BAHNUIK and S. WANG, NASA TM 81747 (1981) p. 1.
179. A. J. WEIGAND, *J. Vac. Sci. Technol.* **15** (1978) 718.
180. H. WOLF, K. DOMASCH, H. J. BRAUER *and* A. VOIGT, *Biomater.* 4 (1983) 289.

Received 9 July
and accepted 11 October 1984